Response to the reviewers

We are grateful to the Editor and the two Reviewers for their precious times in reviewing our manuscript. The comments and suggestions of the Reviewers are very helpful and valuable. The issues raised by the reviewers have been addressed (in blue color) in the revised manuscript. Kindly find a point-by-point reply to the issues as follows (presented in blue color).

Reviewer #1:

1. Fig. 1b presents the SD of AOD, does it the SD mean Shandong province? It is confused.

   Response: Thank you for your nice reminder. The SD presented in Figure 1b means the standard deviation of AOD and has been corrected in the revised manuscript.

2. Annual variations of AOD were shown in Fig.2. More explanations should be given to discuss the reasons.

   Response: Thank you for your important suggestion. In the revised manuscript, two data sets are combined to explore the reasons for annual variations. One is the MODIS fire product that shows the sudden increase in pollution emissions caused by biomass burning in areas. The other is the relative humidity and wind speed issued by NCEP, which may influences AOD via light extinction efficiency of aerosols and modulates the distribution of pollutants. It is found that interannual variation of fire number and relative humidity in the East China are weakly correlated with that of the AOD, However, the interannual variation of the wind speed in lower troposphere was significantly correlated with that of the AOD at 95% confidence level. This implies that the movements of air in vertical and horizontal directions play key roles for the variation of the AOD in the East China in the interannual scale. Therefore, the synoptic patterns were focused. Please find the detailed discussions in the revised manuscript.

3. Fig. 4 and Fig. 5 discussed the two types of air pollution. More discussions should be given how the surface, 850 hPa and 500 hPa circulation match each other to induce the worst air quality or lead to clean air. Temperature contours were also shown, how the temperature influence the AOD distribution?

   Response: Thank you very much for your suggestion.

   (1) The different circulations corresponding to the two typical cases can cause opposite diffusion conditions in vertical and horizontal direction.

According to your suggestion, in the revised manuscript, the vertical velocity and divergence of winds are quantitatively depicted to show the relationship of atmospheric circulation with the AOD distribution in the Figure 5 and Figure 6.

(2) How the temperature influenced the AOD distribution is not easily obtained in this manuscript. It seems that the warm and cold air flows may have such influences. In our work, the temperature field is mainly used to indicate if there are frontal activities in the East China. We found cold front systems in one typical type. In the future, how the temperature is influenced by the AOD distribution will be investigated from view of radiation.

4. It is better to add the emission inventory in the MS in order to show the relationship between AOD and emission distribution.

Response: Many thanks for your nice suggestion. We really want to show the emission distribution in the East China. Unfortunately, the emission data is not available for us in short time. But the previous studies may help us to illustrate the relations between the AOD and the emission distribution. Actually, the AOD data are widely used to enhance the understanding of variations in air quality in local or regional or global scales due to their sensitivity to total abundance of aerosols (Chu et al., 2002; Al-Saadi et al., 2005; Lin et al., 2010). For example, Xin et al (2014) investigated the relationships between daily observed PM2.5 concentration and aerosol optical depth (AOD) in China, they pointed out that there was a high correlation between the two variables, the MODIS AOD are valuable and capable of retrieving the surface PM2.5 concentration as the linear regression function and the correlation coefficient square is R^2=0.57 in autumn (Fig. 1A). Therefore, the AOD are applicable in Chinese regions to characterize aerosol distributions.

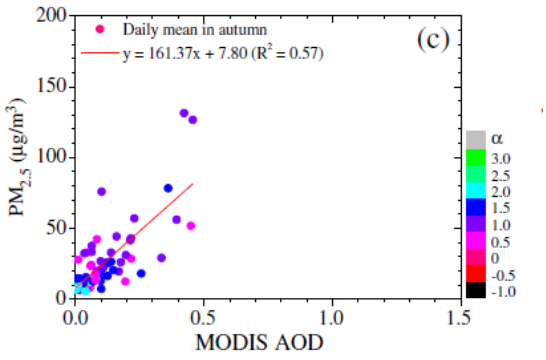

Fig. 1A: The scatterplots and the relationships between the PM2.5 concentration and the MODIS AOD at 550 nm in the autumn. (From: Xin et al, 2014)

5. Six atmospheric patterns were summarized for polluted episodes. The MS only simply described the phenomena according to the figures. More quantified index should be used to indicate the difference among the six types.

Response: Many thanks for the valuable suggestion. According to your suggestion, we have tried many indexes and eventually find that the values of vertical velocity and divergence of wind field are two optimum indexes to compare the differences in diffusion conditions for each type quantitatively. However, it is indeed difficult to find a quantified index to indicate all differences in atmospheric patterns, such as the diverse position of the weather system, the various direction of wind and so on, therefore, the schematic diagram (Figure 17) are combined in the revised manuscript to clearly show the characteristics of the general circulations, so that the readers can easily identify the differences between the patterns by those indicative marks.

6. Vertical structure should be shown to explain the influence of circulation.

Response: Thank you for your very important suggestion. Based on your request, the vertical cross section of vertical velocity and divergence of wind have added in the revised manuscript (Figure 1, Figure 5-6, Figure 8-16) to address the vertical movement of air flows and convergence of winds on each level. The results show uniform descending flows prevails in the East China, moreover, the degree of the pollutant accumulation in the lower atmosphere is determined by the intensity of downward flows. Therefore, the divergence of wind field at different layer plays a key role in determining the column AOD. In the revised manuscript, the corresponding discussions can be found in Section 3 and 4.

Reviewer #2:

Major concerns:

1. The patterns of circulation are not clear to me although it is stated that each type represents specific weather pattern associated with lower and upper atmospheric circulation. The authors should add some schematic highlights (arrows or other indicative marks in Figures 4, 5, and 7-15, so that the readers can identify easily the differences between the patterns listed in Table 1.

Response: Thank you very much for your important suggestion. According to your suggestion, the schematic diagram which clearly show the general circulation characteristics of nine types are presented in the revised manuscript, the indicative marks in different colors represent for the weather system at different layer in the corresponding figure which is named as Figure 17.

2. Accumulation of air pollutants depends on the convergence of winds and the stable atmosphere that does not favor the outflow of air pollutants. The manuscript lacks such information in their analyses.

Response: Many thanks for your crucial suggestions. Based on your request, the vertical cross section of vertical velocity and divergence of wind have added in the revised manuscript (Figure 1, Figure 5-6, Figure 8-16) to address the vertical movement of air flows and convergence of winds on each level. The results show uniform descending flows prevails in the East China, moreover, the degree of the pollutant accumulation in the lower atmosphere is determined by the intensity of downward flows. Therefore, the divergence of wind field at different layer plays a key role in determining the column AOD. In the revised manuscript, the corresponding discussions can be found in Section 3 and 4.

Minor concerns:

1. Line 9 of Page 3287: There should be a '.” after 'factors'.

Response: Thank you for your nice reminder. We have corrected in the revised manuscript.

2. Line 12 of Page 3287: It is not right to say that meteorological parameters are under the control of circulation. For example, atmospheric circulation is influenced by temperature gradient.

Response: Thank you for your reminder. We have corrected in the revised

manuscript that meteorological parameters are closely associated with the circulations.

3. Last paragraph of Page 3287: The authors chose to study for October. Some background information should be given here: Usually what are the most polluted months among a year based on the measurements from other approaches? Is October the worst month or a relatively clean month? How about relative humidity in October since AOD is examined in this work.

Response: Thank you for these important suggestions.

(1) Due to the ground-based observational data in most area of East China are unavailable, we take Anhui Province in East China as an example to show the pollution level of each month based on the measurements from 80 meteorological observation stations. According to Yang et al (2013), the occurrence of haze, i.e. the frequent of haze, reached the maximum in October. Besides, according to Fig. 1A (1b), the visibility in October haze day (5.4km) is the lowest during the autumn. Consequently, October is a relative worse month. Since we focus on the season of autumn, October is undoubtedly selected as a representative month for investigation. The above discussion has been added in the last paragraph of the first section in the revised manuscript.

(2) We have added the information of relative humidity in Figure 2b in the revised manuscript. In Figure 2b, the relative humidity is around 55% for all years except 2001 and 2009, namely, the variation of the relative humidity is not evident. Furthermore, as demonstrated by Twohy et al (2009), the elevated relative humidity can cause an increase of the AOD owing to its impacts on hydrophilic aerosols, whereas the correlation efficient between relative humidity and AOD is -0.4 during the study time and is not significant at the 0.1 significance level.

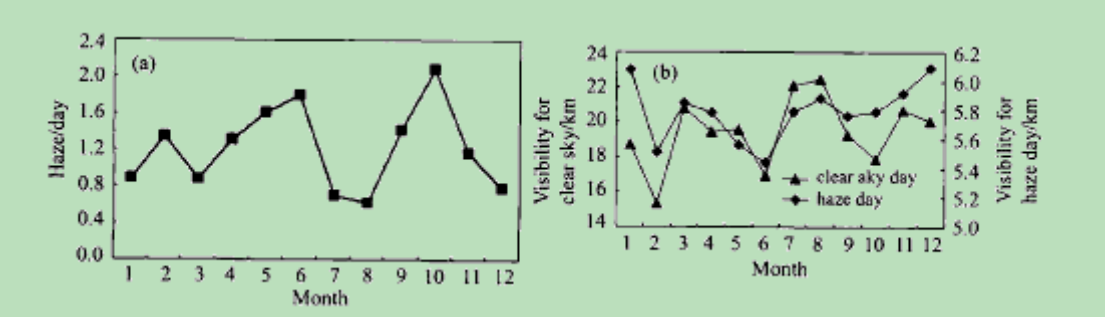

Fig 1A: The (a) number of haze day and (b) visibility for clear/haze day in each month averaged from 2001 to 2009 (From: Yang et al, 2013)

4. Line 16 on Page 3291: What do you mean by 'stable correlation'? Explain.

Response: Thank you for the comment. Sorry for the ambiguous "stable correlation". In the revised manuscript, "close correlation" is used to describe the

relationship between the SLP (sea level pressure) and surface meteorological factors.

5. Line 26 on Page 3291: What are the approximate concentrations of PM2.5 that correspond, respectively, to AOD values of 0.6 and 0.4 in October?

Response: Many thanks for your suggestion. As shown by Xin et al (2014), there is a high correlation between the daily observed PM2.5 concentration and aerosol optical depth (AOD) in North China, and the MODIS AOD were valuable and capable of retrieving the surface PM2.5 concentration as the linear regression function. Fig. 2A describes the linear regression function of autumn, and the correlation coefficient square R^2 is 0.57. According to the linear regression functions of the monthly PM2.5 concentration (y) with the MODIS AOD (x): y = 161.37x + 7.80, when x=0.4, then y=72.34 and when x=0.6, then y=104.62, these two values corresponds to Moderate and Lightly Polluted respectively (as seen in following Table 1A). These also confirm that the definition of the AOD threshold is suitable for our study.

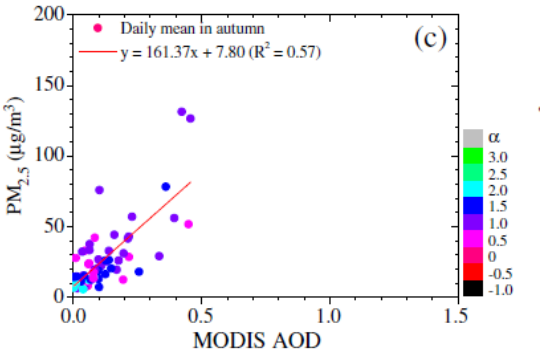

Fig. 2A: The scatterplots and the relationships between the PM2.5 concentration and the MODIS AOD at 550 nm in the autumn. (From: Xin et al, 2014)

AQI	$PM_{2.5}$(ug/m^3)	Pollution level
0-50	0-35	Good
50-100	36-75	Moderate
100-150	76-115	Lightly Polluted
150-200	116-150	Moderately Polluted
200-300	151-250	Heavily Polluted
>300	>250	Severely Polluted

Table 1A. Air quality CLASS

6. Caption of Figure 1 needs to be rewritten. Otherwise it reads as the mean distribution of (b) SD of AOD.

Response: Thank you for your nice reminder. We have corrected in the revised manuscript.

7. Lines 15-17 of Page 3293: Biomass burning can increase AOD because of the enhanced emissions. Such pollution can be identified from AOD but may not be caused by circulation. Does this influence conclusions from this work?

Response: Thank you very much for the important comment. Generally, temporal and spatial variation of the distribution of the AOD is controlled by synoptic patterns and the distributions of emission sources. In this manuscript, we suggested that the anthropogenic emissions are quasi-stable in the East China based on results issued by Xu et al. (2011) that the anthropogenic emissions of widespread pollutant sources are almost constant during a given season in China. As for the biomass burning generated by rural fires, our studies show that it does not influence the interannual variation of the AOD (Figure. 2b). For nine types concluded in the manuscript, we compared the types with almost same fire numbers to reduce the sudden influences from biomass burning and confirm the impacts of atmospheric condition, which added the in the revised Discussions and Figure 18. So, such pollution caused by the biomass burning in rural areas in the East China does not influence the conclusions from our study.

8. Line 21 of Page 3292: Fig 1c actually shows clock-wise winds over selected region.

Response: Thank you for your careful reminder. We have corrected in the revised manuscript.

9. For the purpose of this work, it will be more interesting to show interannual variations in Fig 2b by giving daily AOD so that the readers can see year-by-year variation in pollution events.

Response: Many thanks for the valuable suggestion. According to your suggestion, we have changed daily AOD anomaly to the daily AOD in Figure 2a.

10. English needs to be improved; Chinese style English can be seen in many places throughout the manuscript.

Response: Thank you for your nice reminder. We have corrected in the revised manuscript.

Impacts of Atmospheric Circulations on Aerosol Distributions in Autumn over East China: Observational Evidences

Xiao-Yi Zheng[1] Yun-Fei Fu[1,2,3] Yuan-Jian Yang[1,3] Guo-Sheng Liu[1,4]

1. School of Earth and Space Sciences, University of Science and Technology of China, Hefei, 230026, PR China;

2. State Key Laboratory of Severe Weather, Chinese Academy of Meteorological Sciences, Beijing, 100081, PR China;

3. Key Laboratory of Atmospheric Sciences and Satellite Remote Sensing of Anhui Province, Anhui Institute of Meteorological Sciences, Hefei, 230031, PR China;

4. Department of Meteorology, Florida State University, Tallahassee, FL 32306-4520, USA

Corresponding author address:

Yunfei Fu

School of Earth and Space Sciences, University of Science and Technology of China, Hefei, 230026, PR China

Phone: 86-551-63606897; Fax: 86-551-63606897

E-mail: fyf@ustc.edu.cn

Submitted to *Atmospheric Chemistry and Physics*

ABSTRACT

Regional heavy pollution events in East China (110°E-122°E, 28°N-40°N) are causing serious environmental problems. Pollutants emission due to human activity associated with high urbanization and rapid economic development are considered as an important cause. However, appropriate weather condition is another causing factor which should not be ignored. In this study, the relationship between regional pollution status and larger scale atmospheric circulations over East China in October is investigated using ten-year (2001-2010) MODIS/Terra aerosol optical depth (AOD) product and the NCEP reanalysis data together with case analysis and composite analysis. Generally, statistics in East China show values of mean AOD vary from 0.3 to 0.9 in October over the region, and larger AOD variances are accompanied with the distribution of higher average AOD. Eighteen pollution episodes (regional mean AOD>0.6) and ten clean episodes (regional mean AOD<0.4) are selected and then categorized into six polluted types and three clean types, respectively. Each type represents different weather pattern associated with the combination of lower and upper atmospheric circulation. Generally, the uniform surface pressure field in East China or steady straight westerly in middle troposphere, particularly the rear of anticyclone at 850hPa, are typical weather patterns responsible for heavy pollution events, while clean episodes occur when strong southeastward cold air advection prevails below the middle troposphere or air masses are transported from sea to the mainland. Furthermore, since uniform descending motion prevails over the region, which gather pollutants together in the lower layer, the value of vertical velocity

averaged from 1000hPa to 100hPa and divergence of wind field in lower troposphere are used to quantitatively compare the diffusion conditions in each circulation type. The results reveal that it is usually an clean episode when both the mean downward motion of air currents and divergence of low level winds are strong, which are large than 2.56×10^{-2} Pas^{-1} and $1.79\times10^{-2}s^{-1}$ respectively, or else it is more likely to be a pollution episode. The above studies are especially useful to the government decision making on balance of economic activities and pollution mitigations.

Key words: East China, AOD, atmospheric circulations, pollution episodes, clean episodes

1. Introduction

Concerning that aerosols can perturb the radiation budget of the earth-atmosphere system, influence the climate, and degrade air quality (Kaufman et al. 2002), they have attracted high attention for a long time (Twomey 1977; Rosenfeld et al. 2004; Zhao et al. 2006a, 2006b; Rosenfeld et al. 2007; Li et al. 2011; Koren et al. 2012; Zhao et al. 2012; Zhao et al. 2013a, 2013b; Chen et al. 2014). Particularly, with the rapid urban growth and development of various industries during last decades, the high concentration of atmospheric pollutants has become one of the major environmental problems which usually pose threats to human health (Donaldson et al. 2001; Kan and Chen 2004; Janssen et al. 2011). However, appropriate weather condition is another factor which should not be ignored for these environmental problems (Zhao, et al., 2010; Xu et al., 2011). Therefore, to understand the

mechanisms that control spatiotemporal distribution of aerosols, extensive investigations have been carried out to study the relationship between the air quality and multiple factors. Generally, although the characteristics of regional air quality over a region depend on many complex elements, the major contributions are the emission of the pollutants together with large scale meteorological conditions (Chen et al. 2008a; Chen et al. 2008b). Ziomas et al. (1995) pointed out that in an urban environment, the serious air pollution episodes are not attributed to sudden increases in the emissions of pollutants but caused by meteorological conditions which are unfavorable for dispersion. Normally, the anthropogenic emissions of widespread pollutant sources are quasi-stable in East China, air pollution status here is subject to large scale atmospheric conditions to a great extent (Xu et al. 2011). In some other regions, strong links between the concentrations of aerosols and certain synoptic weather conditions have already been identified (Demuzere et al. 2009; Saavedra et al. 2012). It has also been revealed that under the circumstances of the same pollutant emission quantity, the ground concentrations of pollutants vary directly with different synoptic patterns (Wang et al. 2001).

In fact, the weather condition which consists of a number of meteorological parameters (wind speed and direction, temperature, relative humidity, precipitation etc.) and synoptic patterns analyzed in terms of atmospheric circulations, can contribute to the vertical redistribution and long-range transport of air pollutants leading to an accumulation or a dispersion of aerosols (Cheng et al. 2007; Ding et al. 2009). A growing body of research is showing the important effects of weather

conditions on distribution of pollutants and atmospheric pollution levels. For example, Tanner and Law (2002) investigated the impacts of meteorological parameters (wind speed, wind direction, temperature, relative humidity and solar radiation intensity) on the frequency of high-level pollution episodes in Hong Kong. Ding et al. (2004) successfully simulated the wind patterns of sea-land breezes and the planetary boundary layer (PBL) heights to illustrate the meteorological cause of the photochemical ozone episode, which is associated with Typhoon Nari, in the Pearl River Delta of China. They contrast the characteristics of dispersion and transport on pre-episode and episode days. Xu et al. (2011) confirmed the deterministic impacts of wind speed and wind direction on the concentration of various trace gases at a suburban site between 2 mega-cities. Csavina et al. (2014) examined dust events in two semi-arid sites, and then showed a complex, nonlinear dependence of PM_{10} on wind speed and relative humidity.

The synoptic scale circulations represent a certain atmospheric conditions at a given region through its close association with various meteorological parameters such as wind speed, wind direction, temperature, etc. (Shahgedanova et al., 1998; Kassomenos et al., 2003;Chen et al.,2009). Consequently, instead of using different kinds of weather factors, some relevant studies that used atmospheric circulation patterns have been carried out. For example, Shahgedanova (1998) employed components analysis and cluster analysis for Moscow to develop seasonal synoptic indices which can examine weather-induced variability in CO and NO_2 concentrations, they concluded that anticyclonic conditions in spring, summer and autumn are

introductive to high pollution levels. Flocas et al. (2008) assessed the circulation patterns at the mean sea level for a period of 15 years and distinguished four synoptic scale types, they found the presence of an anticyclone accounted for highest percentage of pollution episode over Greece. Moreover, Zhang et al. (2010) used numerical mode method to simulate the impacts of weak/strong monsoon circulations on interannual variations of aerosols over eastern China under the conditions of same anthropogenic emissions, they suggested that the decadal-scale weakening of the East Asian summer monsoon is responsible for the increase in aerosol concentrations over eastern China. By using independent satellite products, Zhao et al. (2010) showed consistent disappearance of CO and O_3 enhancements over southeastern China at the onset of East Asian summer monsoon and reemergence after the monsoon wanes, these confirmed strong modulation effects of monsoon system on regional air quality. Liu et al. (2013) further demonstrated a potential influence from the variation of large-scale circulation, El Nino Southern Oscillation, upon the interannual fluctuation of summertime aerosol optical depth (AOD). Russo et al. (2014) applied the analysis on 10 basic circulation weather types characterized through the use of a set of indices, and their results showed that easterlies prevailed during pollution episodes of three pollutants (NO_2, PM_{10}, O_3) in Portugal.

The aforementioned works suggest that synoptic types play a crucial role in the formation of a pollution episode, they established predictive connection between air quality and circulation patterns over various regions, and provided valuable scientific basis for weather forecast operation. To the authors' knowledge, even though some

attempts have been conducted to study the similar relationships in China , most of them chose to study a single city (Wang et al 2007, Chen et al. 2008b, Guo et al 2013) rather than a regional scale area (e.g., East China in this study). East China, as a highly urbanized region, with rapidly increasing of industrial and automotive emissions, is frequently characterized by poor air quality (Ding et al., 2008; He et al. 2012). Therefore, the understanding of a predictable relationship between circulation patterns and air qualities is considered significant for the quick indication of the pollution episodes.

In present study, we evaluated the above relationship during autumn using ten-year (2001-2010) MODIS/Terra aerosol optical depth (AOD) product and atmospheric circulations of NCEP reanalysis data. The choice of autumn is in consideration of the following reasons. First, in contrast with other seasons, the local atmosphere structure of autumn is more stable and mainly influenced by the large-scale synoptic system, the dynamic impact is stronger than the thermal effect. These features reduce the influence of complex mesoscale weather systems and small-scale weather disturbances, thus more suitable for the study of large-scale atmospheric circulations. Second, the wet deposition effect is weaker due to the less precipitation in autumn (Chen et al. 2012), which also ensures the availability of AOD data. Finally, previous researches rarely focused on the pollution episodes during autumn. In addition, Anhui province is taken as an example to show the pollution level of each month in East China (Yang et al., 2013), the occurring frequency of haze day for Anhui is the highest in October during a whole year, based on the

measurements from 80 meteorological observation stations. Therefore, October is selected as a representative autumn month for our present work. The paper is organized as follows: a brief introduction of the data and processing methodology used in this study is presented in section 2. In section 3 and 4, we describe the interannual variability of AOD over East China and then extend our exploration to the relationships between AOD and characteristics of synoptic circulations through statistical and synthetic analysis. After that, conclusions are given in section 5, in which general characteristics of various types associated with different spatial distributions of AOD over East China are summarized.

2. Data and Methods

Data used in this study and methods for sampling high/low AOD cases are described in this section. The research considers the period from 2001 to 2010 and the region between 110°E to 122°E, 28°N to 40°N.

2.1 Pollution data

The main data set used to describe air quality is the daily averaged Collection 5.1 level 3 AOD products (at 1 degree horizontal resolution) which are derived from the Terra's Moderate-resolution Imaging Spectroradiometer (MODIS), data products are accessible at http://ladsweb.nascom.nasa.gov/data/search.html. Compared to the ground based data, MODIS provides long-term continuous observations for the spatial and temporal distribution of aerosol, which is convenient for developing multi-aspect researches. AOD is the degree to which aerosols prevent the transmission of light by scattering or absorption effect. By using the MODIS/Terra aerosol data, Kim et al.

(2007) evaluated the temporal and spatial variation of aerosols over East Asian. Wu et al. (2013) pointed out that MODIS data were usually valid throughout China and then revealed characteristics of aerosol transport and different extinction features in East Asia. Luo et al. (2013) identified the well performance of MODIS AOD over land in China and they used 10 years data to construct the climatology of AOD over China. According to previous validations, MODIS AOD data are applicable in Chinese regions and can capture the aerosol distributive characters.

Actually, the AOD data are widely used to enhance the understanding of changes in air quality over local, regional, and global scales as a result of their sensitivity to total abundance of aerosols (Chu et al. 2002; Al-Saadi et al. 2005; Lin et al.2010). AOD can indicate the air quality to a certain degree, the higher the AOD value is, the worse air quality becomes (Liu et al. 2013). In this study, we discuss the cases of pollution and clean separately.

Finally, the Collection 5 MODIS active fire product (MCD14ML) are used to monitor the influences of the sudden enhanced emissions from biomass burning. The monthly fire location product contains the geographic location, date, and some additional information for each fire pixel on a monthly basis. The Terra-observed pixels whose detection confidence is greater than 60% are used from 2001 to 2010.

2.2 Meteorological Data

The corresponding atmospheric fields analyses performed in this paper are based on the results of meteorological reanalysis products made available by the National

Center for Environmental Prediction (NCEP) and National Center for Atmospheric Research (NCAR). For a complete discussion, we consider both surface and upper-air circulation patterns. The sea level pressure (SLP) field, which is closely related to the meteorological factors, is selected to characterize a certain synoptic episode. Besides, the 850hPa level and 500hPa level are selected as the typical height of lower and middle troposphere, respectively. Mean sea level pressure and temperature at surface and the 500hPa level, geopotential height at the 850hPa and 500hPa level, along with relative humidity, wind field and vertical velocity were extracted from NCEP/NCAR Reanalysis dataset on a $2.5^{o} \times 2.5^{o}$ latitude/longitude grid on a daily basis (http://www.esrl.noaa.gov/psd/data/gridded/data.ncep.reanalysis. html).

2.3 Methods

On the basis of ten-year October data, namely 310 days, we get the daily AOD distribution. According to the threshold of AOD (mentioned in section 3.1), the whole 310 days are divided into four categories: high AOD (>0.6), low AOD (<0.4), median AOD (0.4~0.6) and the missing-value day (due to clouds). Ignoring the group of missing and median data, the circulation fields correspond to the other two categories (high AOD and low AOD) are evaluated at the same time. Since satellite-based AOD exists certain uncertainties, therefore, the consecutive days of high (or low) value can better illustrate the existence of the air pollution than just one day. And statistical results of two categories also show that the occurrence of high (or low) value of AOD inclined to last for several days. Besides, the corresponding circulation pattern is also quasi-steady during these high (or low) AOD periods.

Taking the above facts into account, the first synthetic process are conducted by averaging the corresponding grid point values for successive days (greater than or equal to 2 days) presented as high(or low) AOD. Following this approach, 28 episodes, among which there are 18 high-value episodes (HEs) and 10 low-value episodes (LEs), are initially identified during 2001-2010. In order to obtain the statistical characteristics of the pollution and clean episodes, the second synthetic process is performed. We classify the 18 HEs and 10 LEs obtained in the first step on a synoptic basis and average the similar circulations for these two different categories respectively, a thorough description of results obtained by this method can be found in section 3.3. The 18 HEs are clustered into six types while 10LEs are three types. Thus, nine distinct circulation types are consequently considered in the following analyses.

2.4 Hybird Single-Particle Lagrangian Integrated Trajectory (HYSPLIT) Model

The backward trajectories for two typical episodes discussed in section 3.2 are simulated using the HYSPLIT model, employing NCEP/NCAR reanalysis meteorological data as input fields. With powerful computational capabilities, the HYSPLIT_4 model is a widely-used system for calculating simple trajectories to complex dispersion and deposition simulations using either puff or particle approach (readers are referred to Draxler and Hess (1997) for more detail of the model). Borge et al. (2007) used back trajectories computed with HYSPLIT model to examine the impact of long-range atmospheric transport on urban PM_{10} for three cities. Chen et al. (2013) incorporated eight size PM fractions of metals to the HYSPLIT model and provided a prediction of the size distribution and concentrations of heavy metals. In

this work, the air-mass trajectories are evaluated in order to present the different movement of air parcels during the two contrary episodes.

3. Results

3.1 Climatological mean and interannual variation

Prior to the analysis of the link between air quality and large-scale circulations, it is necessary to reveal the backgrounds that climatological mean and interannual variation of AOD in October over East China. The climatological mean AOD from MODIS are obtained for the period from 2001 to 2010. As shown in Figure 1a, the spatial distribution show AOD ranges from 0.3 to 0.9 for almost the entire area. Four prominent centers of high AOD values are found in East China, i.e., Bohai Gulf, Yangtze River delta, junctional areas of Anhui, Shangdong and Henan provinces, and most parts of Hubei and Hunan provinces which were recognized as the source of high emissions in October according to Wang and Zhang (2008). In other words, these centers are considered as possible consequences of industrial emissions or agricultural biomass burning which occurs in autumn with certain meteorological conditions. Figure 1b presents the standard deviation of AOD for the same period. The distribution pattern of Figure 1b is similar to that of Figure 1a, which means the standard deviation is larger over the region where the mean AOD is higher. Moreover, the climatological mean wind vectors at 850hPa and geopotential height are shown in figures 1c and 1d. Obviously, weak clockwise winds at 850hPa (Figure 1c) and flat western flow at 500hPa (Figure 1d) level suggest that East China is dominated by the large-scale stable circulation without the frequent disturbances of small-scale weather

systems. As for vertical structure, figures 1e and 1f present height-latitude cross-sections of vertical velocity and divergence of wind respectively. In figure 1e, the positive value indicates uniform descending motion over the East China. Figure 1f also shows convergence in upper altitude and divergence in lower altitude, which are favorable to the maintenance of downward atmospheric motion. Interannually, we show ten-year distribution of AOD over East China in October (spatial distribution in Figure 2a and regional mean in in Figure 2b).

As indicated by Ziomas et al. (1995) and Xu et al. (2011), in a given season, the anthropogenic emissions are almost constant, however, the biomass burning in rural areas may cause a sudden increase in pollution emissions. Consequently, we combine MODIS fire product with NCEP relative humidity which could influence AOD via light extinction efficiency of aerosols and wind speed that may modulate the concentration of aerosols to explore the annual variations. As shown in figure 2b, it is found the interannual variation of fire number in the East China is weakly correlated with that of AOD. For example, the AOD of 2003 is lower than 2006 but fire number is larger. It implies that there are other factors contributed to the variation of AOD. For the relative humidity, it is around 55% for all years except 2001 and 2009, namely, the variation of the relative humidity is not obvious. Furthermore, as demonstrated by Twohy et al (2009), the elevated relative humidity can cause an increase of AOD owing to its impacts on hydrophilic aerosols, whereas the correlation coefficient between relative humidity and AOD is -0.4, which did not passed over 90% confidence level. However, the relationship between wind speed and AOD is negative

(-0.63) at 95% confidence level, which demonstrates that decreasing values of AOD occur with increasing values of wind speed. Based on the above results, it is deduced that the interannual variation of AOD in East China, to a certain extent, is determined by the vertical and horizontal movements of air flows, which can influence the spatio-temporal distribution of aerosols.

In order to depict the frequency of pollution event and give the threshold beyond which the value can be regarded as high AOD, we count the frequency distribution of high AOD(>0.5 and >0.6) plotted in Figure 3. Luo et al. (2014) considered the value of AOD>0.5 as the high value in China. However, for more than half of East China, it is found that the frequency of AOD>0.5 is larger than 50% (Figure 3a). Consequently, we define 0.6 as the rigor critical value. Compared to Figure 3a, the area with relative high frequency reduces in Figure 3b, and the frequency of above 65% area of East China is less than 50%.On the contrary, the day is classified into the low-value group on condition that the value of regional mean AOD over the study area is less than 0.4. Xin et al (2014) investigated the relationships between daily observed PM2.5 concentration and aerosol optical depth (AOD) in North China, they pointed out that there was a high correlation between the two variables in autumn for that the correlation coefficient square R^2 is 0.57, and the MODIS AOD were valuable and capable of retrieving the surface PM2.5 concentration. According to the linear regression functions pointed by the research, when AOD is 0.4 (0.6), the $PM_{2.5}$ concentration is 72.34 ugm^{-3} (104.62 ugm^{-3}), these two values correspond to moderate and lightly polluted in China, respectively, and these also confirm that the definition

of the AOD threshold is suitable for our study. Furthermore, according to the topography shown in Fig 3c, it is evident that the emergence of high frequency is related closely to the terrain of East China. It notes that the pattern of high frequency distribution (Fig 3b) is consistent with that of high values of ten-year mean AOD distribution (Fig 1a). High AOD mainly concentrated in plain and hilly areas, especially the economically developed Yangtze River Delta, which are characterized by dense population along with a great number of industrial and vehicle emissions.

Since MODIS-AOD represents for the aerosol column abundance rather than the content of pollutants mere near surface, the upward motion alone in vertical direction which favors the diffusion of pollution cannot change the value of AOD. Moreover, the aforementioned two vertical cross-sections illustrate that the climatological mean vertical velocity in autumn East China averaged from 1000hPa to 100hPa is downward of 2.56×10^{-2} Pas^{-1}. This suggests that the strong downdraft leads to a more concentrated vertical distribution of pollutants, which gather pollutants together in the lower layer. As a result, AOD will mainly depends on the divergence of low level wind field in autumn East China. The severe divergence of wind field in the lower troposphere facilitates the diffusion of aerosols, whereas the weak divergence favors the formation of poor air quality. As shown in Figure 1f, the climatological mean divergence, averaged from 1000hPa to 850hPa, of lower troposphere is $1.79\times10^{-6}s^{-1}$.

The relationships among the AOD and vertical velocity and divergence during the study period was shown in the scatter diagram (Figure 4a). According to the climatological mean of vertical velocity and the low level divergence, we divide the

sample into four categories: C1, C2, C3, C4. There are significant differences in vertical velocity and divergence between the distribution of high AOD group and low AOD group. For example, the group with AOD less than 0.4 mainly distributed in C1, which indicates that both the vertical velocity and divergence are relative strong. The increasing values of AOD occur with decreasing values of vertical velocity and divergence of low level winds, and the bottom-left corner of the figure is primarily occupied by high AOD group. And for a more intuitive performance, Figure 4b shows a histogram of occurrence frequency for high AOD (>0.6) and low AOD (<0.4) group, which correspond to polluted and clean environment, respectively. C1 presents maximum frequency of low AOD group, which is nearly 60%. Conversely, pollution exist predominantly in the categories with weak divergence, especially in C3, where both of two variables are less than the climatological averages. These are consistent with our hypothesis and confirm that the mean vertical velocity and low level divergence of winds result from diverse synoptic patterns, are indicative of regional air quality.

3.2 Two Typical Cases: High and Low AOD

On the basis of the above results, two typical cases are presented in this section to show the differences between pollution and clean episodes. The process during 28th-31st October 2006 is analyzed as a typical high AOD episode (HE) example, whereas the 4 days from October 21st to 24th in 2003 are selected as a typical low value episode (LE). First of all, we give the fire numbers of two cases, which are 18 for HE and 25 for LE accordingly. Since the difference of sudden enhanced emissions

from biomass burning between two cases are little, it is can be concluded that AOD might be depended on the atmospheric circulations.

The mean patterns of AOD and atmospheric circulations at surface, 850hPa level, 500hPa level in the period of the HE example are given in Figure 5. The regional average AOD of HE is 0.76 which signified a pollution process, and maximum value was greater than 1.2. The corresponding sea level pressure pattern (Figure 5b) were almost controlled by uniform pressure field without obvious control effect, and the shallow trough promoted west-northwest flow at 500hPa (Figure 5d), which represented a stable synoptic pattern and was conductive to the storage of air pollutants. In vertical direction, the obvious downward motion is in accordance with climatological pattern of autumn (Figure 5e), and whole-level averaged value over East China is $3.67\times10^{-2}Pas^{-1}$, leading to an accumulation of aerosols in low layer. During this period, the main feature of wind filed at 850hPa level was the weak clockwise circulation centered at Shanxi province, wind blew from the north in East China under the control of a large scale anticyclone (Figure 5c). The divergence of winds in lower troposphere is $1.62\times10^{-6}s^{-1}$ for HE (Fig. 5f), which is less than the climatological mean and does not favor the outflow of air pollutants

Figure 6 shows the mean patterns of LE example from October 21st to 24th in 2003. Unlike the polluted episodes (Figure 5a) when the whole East China was masked by high aerosol loadings except a small area in northwest, the area was mainly influenced by low AOD (<0.4) (Figure 6a). And the mean AOD (0.38) was at half the level HE reached. In Figure 6b, the surface circulation of LE in East China

was to the front of the high pressure centre. The temperature and geopotential height in the middle troposphere (500hPa) indicated a dominant northwesterly flow prevailed over East China and led cold air masses to low-mid latitude (Figure 6d). Under these conditions, the vertical velocity of LE (8.05×10^{-2}Pas^{-1}, Figure 6e) is much larger than that of HE over whole vertical layer, which generally results in complete concentration of pollutants and then played an important role in the diffusion of air pollutants when combined with relative strong divergence of winds in low troposphere (2.86×10^{-6}s^{-1}, Figure 6f.), while HE shows clear distinctions, specifically the weaker downward atmospheric motion and adverse divergent conditions. Moreover, compared to the northerly of 1–4 ms^{-1} in HE episode (Figure 5c), stronger northwesterly winds of 6–9 ms^{-1}were observed at 850hPa (Figure 6c).

In addition, to describe different air mass sources and transport path, HYSPLIT model was applied to the days when the two typical episodes occurred. For each day, we calculated the backward trajectories originated from three locations and the associated ending height is 1000m above ground level. Trajectories were considered to be initiated at 0200 (UTC) when MODIS/TERRA passes across China, terminating at the end of 48 hours. As shown in Figure 7, the backward trajectories of four polluted day (Figure 7a) were composed of short tracks, which were mainly trapped in East China. This indicated that the pollution was caused by the combination of the circulation pattern which gone against dissipation of air pollutants and a great deal of local emissions in the studied area. In contrast, the LE presents a cluster of relatively longer trajectories corresponded to fast-moving air mass from Mongolia.

Northwesterly cold winds on these days dispersed local air pollutants, and also brought clean air.

3.3 All Selected Cases

The aforementioned case studies show that, without considering the variations in emission, some synoptic types are favorable to the occurrence of the air pollution while others are quite contrary. A comprehensive statistic of all cases in the study period over East China is conducted. Excluding all missing and median days, the total 121 days are extracted for the research, of which there are 90 days with high AOD and 31 days with low AOD. Table 1 and Table 2 list the statistical results of 18 pollution episodes and 10 clean episodes respectively.

It is found from Table 1 that 2002 and 2006 are both years with maximum occurrence (16 days) of pollution, and this is in accord with the high value presented in Figure 2. The estimated duration of pollution episodes, on a daily basis, mostly lasts for about four days or longer. To be more specific, for sea level pressure field, the most frequent pattern is characterized as the periphery of the high pressure centered in the Tibetan plateau or Mongolia, amounts to 38 days. The uniform pressure over the East China is the second high-frequency type with a percentage of 37%, namely 34 days. Among the remaining three types, one is interpreted as the pattern before the passage of a cold front, and the corresponding pattern in lower troposphere (850hPa) is characterized as strong cold air flow moves toward the East China, which involves 2 episodes (6 days). The other 15 episodes are dominated by the anticyclonic circulation in 850hPa, it is noted that the region is controlled by the

different part of anticyclones, the frequency of the rear of anticyclone is 35 days, while the frequency of the foreside and the center of anticyclone are both 23 days. For patterns of 500hPa geopotential height, there are 30 days influenced by the northwest (NW) flow, of which 25 days were caused by the upper air trough. The number of days associated with the west-northwest (W-NW) flow and west (W) flow, is 19 and 7, respectively, in addition, the southwest (SW) flow prevailed during a three-day episode.

Table 2 is same as Table 1, but for 10 clean episodes. According to the Table 2, the number of low-value day peak in 2003.The high pressure centered in the northwest of China on surface is the frequent patterns since it accounts for 15 days of the whole 31 clean days. Besides this, 8 days go through the passage of a cold front and the rear of a high pressure system over the Yellow Sea follows with a frequency of 5 days, the rest 3 days is characterized by the uniform pressure field. For 850hPa wind fields, frequency of the pattern dominated by anticyclonic wind vectors over the study area is the highest, it is 12 days. Secondly, it is the anterior part of anticyclone (11 days) and the rest two episodes related to the upper air cold front bring strong and cold stream southwardly in the lower troposphere. The 500hPa geopotential height of clean episodes, unlike that of pollution episodes, include only two dominant airflow directions. For most of clean days, the northwest flow prevails, whereas the other 5 days are associated with the flat west stream.

The characteristics of circulation patterns of all pollution episodes and clean episodes at each level are gained through the above statistics. In terms of a single

level (surface/850hPa/500hPa), the circulation patterns for different episodes are similar. However, it is the combination of circulations at lower level and upper level that the air quality always depends on. The rows in the Table 1 and Table 2 with same capital letters in the parentheses following the sequence number indicate those episodes are affected by the similar circulation patterns in all the three atmospheric levels. There are nine different letters in two tables, namely, the entire 28 episodes are classified into nine different types, among which there are six pollution types and three clean types.

3.4 Statistics and synthetic analysis

Based on the above results of all cases, nine types are detailedly inspected in this section. Before the description of each type, it is pointed out that the mean AOD and meteorological fields for each type, which consist of the sea level pressure and surface temperature, the 850hPa wind and geopotential height, the 500hPa geopotential height and temperature, the cross-section of vertical velocity and wind divergence, are averaged from the several episodes that marked with same letter in Table 1 (Table 2). The percentage of each pollution (clean) type is calculated on a daily basis. More specifically, Figure 8-13 presents the spatial distribution of mean AOD for six high-value types and the associated large-scale three-dimensional atmospheric circulation structure. Each type contains a set of three different layers and differs from each other, either in terms of the position and intensity of weather systems or in the vertical allocation of the corresponding atmospheric circulations.

Firstly, the two episodes marked with the letter A in table 1 are classified as type 1, which account for 6.7% of all polluted days. Distribution of AOD is shown in Figure 8a, high value appeared in Anhui province and the regional mean AOD is 0.60. The corresponding atmospheric circulations were shown in Figures 8b-8d. In detail, the sea level pressure field is characterized as the pattern before the passage of the cold front. Before the arrival of cold flow caused by the low-pressure system over northeast of China, warm air mass accumulates ahead of the front, which favors the increase of pollutants. At higher layer, the area is situated behind the trough, and thus the dominant wind direction in the East is northwest, which gradually leads cold air that mixed with northern pollutants toward the East China. Even though the vertical downward motion is strong (5.13×10^{-2} Pas^{-1}), the divergence of winds in lower troposphere is weak ($0.49\times10^{-6}s^{-1}$), in fact, the convergence of air at 850hPa can be seen in Figure 8c, whereas the wind speed is relative high. In view of the above-mentioned facts, the pollution of this type is not quite serious.

Type 2 (marked with the letter B) is the most frequent among the six polluted types with a percentage of 40%. It is evident that the occurrence of pollution in East China mainly requires a uniform pressure field on surface (Figure 9). At 850hPa level, the pattern corresponds to weak southerlies for it is controlled by the rear sector of an anticyclonic circulation. Besides, the upper west-northwest flow is crossing the area. Under those fair weather conditions, both the vertical velocity ($1.97\times10^{-2}Pas^{-1}$) and divergence ($0.97\times10^{-6}s^{-1}$ for lower troposphere and $1.08\times10^{-6}s^{-1}$ for middle level), for type 2 are less than the climatological mean mentioned before, allowing the

stagnation of pollutants. According Table 1, it seems that type 2 can last for a long time. Generally speaking, type 2 is a relatively stable and serious pollution example with a mean AOD value of 0.77.

Type 3 (marked with the letter C) is associated with four episodes, accounting for 21.1%. From Figure 10a, high values center in Henan province, extending to the southeast and southwest. The circulation structure, corresponding to this type, is shown in Figure 10b-10d. On the surface, the region is governed by the periphery of a high pressure system located in Mongolia, which results low pressure gradient over the central of East China. At 500hpa, an upper air trough cause moderate northeasterly flows, the wind field in lower troposphere can be considered as anticyclonic and the wind direction is consistent with the direction of diffusion of pollutants. From Figure 10e, the strong descending motion promote, which is 4.91×10^{-2} Pas^{-1}. However, the limited low level speed and divergence of winds ($1.54\times10^{-6}s^{-1}$), prevent the spread of pollutants to the outside area. These conditions yield a regional average AOD value of 0.61.

Type 4 (marked with the letter D) consists of four pollution episodes (accounts for 18.9%), which all last for 3 to 5 days. It resembles Type 2 concerning the spatial distribution of AOD (Figure 11a), but the contamination degree of type 4 is relatively light and mean AOD is 0.63. On the surface (Figure 11b), the pattern is characterized by the periphery of a high barometric system, which lies over Tibetan Plateau. The lack of pressure gradient allows for formation of pollution. At 850hPa (Figure 11c), an anticyclone centered over the study area, results to moderate to low wind speed. In the

middle troposphere, the circulation is almost zonal passing through mid-latitudes (Figure 11d). Compared with type 2, the vertical velocity and the divergence which are respectively shown at Figure 11e and 11f over East China are stronger. Nevertheless, it should be noted that low-level averaged divergence is relative weaker to that of climatological mean. And maybe these are why the mean AOD of type 4 is less than type 2.

Type 5 (marked with the letter E) depicts a different pattern of pollution distribution. As shown in Figure 12a, the main difference between these types is that, for type 5, the pollutants gather in the northeast other than the center of the studied area. Because of the relative concentration of pollution, the regional mean AOD reach 0.60 merely. Figure 12 represents the associated circulations. On both surface and 850hPa level, East China is found in a rear zone of the high pressure systems, located in eastern ocean. The southerly wind dominates in the lower troposphere, while in the middle troposphere, the sparse isopleths indicate small geopotential height gradient. Owing to the handicap in vertical motion (2.21×10^{-2} Pas^{-1}) and also in the divergence of winds ($1.64\times10^{-6}s^{-1}$) under such calm weather condition, the pollution is formed. This type occurred on 10% of all polluted days in the sample.

Type 6 (marked with the letter F) consists only one 3-day episode (accounts for 3.3%). Very high values are found in Hunan province and average AOD of the whole area is 0.70. A surface high pressure system centered over the Yellow Sea, results to southerly flow over the East China, which also prevails in the lower troposphere. These conditions also contribute to the northward extension of pollutants (Figure 13a).

As shown in Figure 13e, the vertical velocity pattern is different from that of other pollution type. The descending motion is prevailed in the vertical direction, except for lower troposphere, transporting some pollutants to higher level. Consequently, we consider the divergence of both low and middle troposphere that presented in Figure 13f. Despite the divergence of low level is $2.63\times10^{-6}s^{-1}$, the corresponding value of middle troposphere is merely $0.72\times10^{-6}s^{-1}$, thereby, the column AOD is large. Generally, type 6 is identified as a "southerly type".

Similar to the pollution episodes, the results for clean episodes are detailed in the following paragraphs. The distributions of AOD and the corresponding weather maps for each clean type are shown in Figure 14-16.

Type 7 (marked with the letter G) is the most frequent clean type during the whole examined low-value days (accounts for 57.6%). As shown in Figure 14a, the maximum AOD is less than 0.6, in addition, the mean AOD for the entire region is 0.33, which represents for improved air quality by contrast with the above polluted types. According to the circulation patterns of type 7 (Figure 14), On the surface, the cold air moves toward the East China continually in front of the high barometric system located in Inner Mongolia. A trough appears in the upper atmosphere, accompanied by an anticyclonic eddy in the lower troposphere, which causes strong northwesterly winds (Figure 14c and d) in the area. When considering the vertical structure of type 7, as shown in LE, uniformly downward motion with the vertical velocity of 5.78×10^{-2} Pas^{-1} prevails. Therefore, strong divergence ($2.93\times10^{-6}s^{-1}$) results from wind field in the lower troposphere facilitate the removal of the accumulational

pollutants from the locality.

Type 8 (marked with the letter H), which accounts for 18.2% of all clean days, is characterized by the rear of weak high pressure system centered in the east coasts of China (Figure 15). In accord with the pattern on surface, anticyclonic conditions are observed in 850hPa. The vertical downward motion (2.65×10^{-2}Pas^{-1}) in the East China is a bit stronger than that of climatological mean, whereas the divergence (3.60×10^{-6}s^{-1}) is much larger compared with ten-year average, blowing away local pollutants and bringing clean air from the sea to the region. The above conditions induced a lower mean AOD value of 0.35.

Type 9 (marked with the letter I) is the cleanest type with an average AOD value of 0.31. It is identified as the passage of a cold front and the associated frequency is 24.2%. On the surface, the high pressure system over the northwest of China, along with a low pressure system centered in northeast of China, intensifies the southward transfer of cold air masses, as it can be seen in Figure 16. In the lower troposphere, strong northwesterly winds prevail in the region, and the dense isopleths which represents for distinct geopotential height gradient, appears in middle troposphere. Strong descending motion (6.81×10^{-6}s^{-1}) is associated with the whole vertical layers of atmosphere while favorable diffusion condition at low layer is shown in Figure 16f. Generally, the advection of cold and dry air from northwest, contributes to the good air quality.

4. Discussion

The above nine general circulation types, which is clearly extracted and highlighted in the schematic diagram of Figure 17, correspond to different level of air quality. In Table 1 and 2, it can be found that two typical cases (HE and LE) correspond to type 4 and type 7 respectively. To assess the relationship between diffusion conditions and synoptic patterns in autumn, the value of vertical velocity averaged from 1000hPa to 100hPa and divergence of wind field in lower troposphere are quantitatively compared among these circulation types (Figure 18). And in this study, the climatological means are used as the threshold to discuss the diffusion ability of environment. In general, when the mean downward motion of air currents is strong over East China and with a value larger than $2.56\times10^{-2}Pas^{-1}$, then the divergence of low level winds is a predominant factor in deciding the column AOD owing to the accumulation of pollutants in low layer. As shown in Fig 18, three polluted types (Type 1, 3, 4), the divergence of which are less than $1.79\times10^{-2}s^{-1}$, and three clean types (Type 7, 8, 9) with favorable divergent conditions are found. However, Type 2, 5 and 6 are recognized as the types with weak downward motion, and the aerosols may not be gathered in the lower level. Consequently, it is necessary to account for the convergence of the middle layer due to its modification on the distribution of upper pollutants. In fact, the convergence in upper altitude and divergence in lower altitude always appear in autumn, this indicate the divergence of upper level winds is usually weaker than that of lower level, or even shows as convergence. For type 2 and type 5, the divergence in middle layer are 1.08×10^{-6} and $0.7\times10^{-6}s^{-1}$ respectively, which implies that the divergence of these two types are poor

at both low and middle level. Type 6 is the one with minimum vertical velocity, actually, the upward motion of air in low troposphere transports pollutants to higher level, and the weak divergence in middle layer ($0.72\times10^{-6}s^{-1}$) leads to the severe pollution.

Admittedly, temporal and spatial variability of air pollution levels are controlled by weather conditions in conjunction with a complex emission framework. In this study, we suggested that the anthropogenic emissions is almost constant in a given season followed by previous studies (Ziomas et al.1995; Xu et al. 2011.). However, the biomass burning in rural areas may cause an increase in pollution emissions. Therefore, to reduce the sudden influences from biomass burning and confirm the impacts due to atmospheric condition, we contrast the types with almost same fire numbers derived from MODIS active fire product. Although the mean fire numbers for type 2, 3 and 7 are nearly equal to each other (28, 31 and 26), their corresponding AOD values are different, which is result from different weather conditions. The diffusion of type 7 is the best while type 2 is the worst in the three types as seen in Fig 18. Similarly, the additional emission from burning is close for type 4, 5, 9 and less than the aforementioned three type since the fire numbers are 20, 15 and 18 in sequence, but the mean AOD of type 9 is merely half of type 4 and 5 owing to its favorable synoptic patterns. In addition, type 6 and 8, with fire number as 9 and 7, respectively, present exactly opposite air quality and the pollution of type 6 is very severe, even if the fire numbers of them are relative small than other types.

5. Summary and conclusion

In the present study, the climatological mean and interannual variation of AOD over East China (110°E-122°E, 28°N-40°N) are investigated through the statistical analysis of ten-year MODIS data (2001-2010). In consideration of weather characteristics of autumn, and slight sudden variations of pollutants emission during a short time, October is selected as typical month to study. The air qualities of total 310 days studied in this paper are represented by the satellite-based AOD and the corresponding meteorological fields are extracted from NCEP/NCAR Reanalysis dataset. In fact, the circulation patterns assessed at the three levels (surface, 850hPa and 500hPa) on the episode days are identified. The main conclusions are summarized as follows.

Firstly, the daily mean AOD value ranges from 0.3 to 0.7 in large parts of the East China except for four widespread high-value centers, which are considered as possible consequences of constant industrial emissions or agricultural biomass burning. The fluctuation is more volatile over the region where the mean AOD is higher. The circulation patterns indicates that the East China is frequently dominated by the large-scale stable circulation in autumn, such as anticyclonic circulation at 850hPa and northwest flow at 500hPa. Furthermore, Since uniform descending motion prevails over the area, which gather pollutants together in the lower layer, the divergence of low level wind field plays a key role in determining the column AOD.

Moreover, two distinct extreme episodes (LE (October 21st to 24th in 2003) and HE (October 28th to 31st in 2006)) are picked to initially examine the relations

between meteorological fields and air qualities. These two episodes showed different circulation patterns at both lower and high level, besides, the features of two sets of backward trajectories supported the distinct distributions of AOD associated with two episodes. In addition, to get a better insight into the impacts of circulation patterns on episodic events over East China, a comprehensive statistic of all 28 episodes occurred in the study period are carried out, among which there are 18 high-value episodes (90 days) and 10 low-value episodes (31 days).

Finally, according to the similarity of circulation patterns for all 28 episodes in all the three levels, the 18 pollution episodes are classified into six types, while the other 10 clean episodes are classified into three types. Each type differs from each other, either in respect to the position and intensity of weather systems or the combination of lower and upper atmospheric circulations. Compared with the polluted types, generally, the flow of the clean types in the both middle and lower troposphere strengthened significantly. These conditions were propitious to the horizontal diffusion of air pollutants. Particularly, patterns that associated with the uniform pressure field in the East China or steady westerly flow in middle troposphere, or the control of an anticyclone are good indications of pollutions, while clean episodes occur when strong southeastward cold air advection prevails below the middle troposphere or air masses are transported from sea to the mainland. And the values of vertical velocity and divergence of wind field are effective indexes to compare the differences in diffusion conditions for each type quantitatively.

In general, the above results have confirmed the impacts of large-scale

atmospheric circulations upon aerosol distributions over East China. Since the empirical classification of weather types are convenient to correlate different circulations patterns with the different air qualities, therefore, these results are valuable as an assistance to the government decision make on balance of economic activities and pollution mitigations.

Acknowledgments This work is supported by CAS Strategic Priority Research Program (Grant XDA05100303), Special Funds for Public Welfare of China (Grant GYHY201306077), the NSFC (Grant 41230419, 91337213 and 41205126), and the Jiangsu Provincial 2011 Program (Collaborative Innovation Center of Climate Change).

References

Al-Saadi, J., Szykman, J., Pierce, R. B., Kittaka, C., Neil, D., Chu, D. A., Remer, L., Gumley, L., Prins, E., Weinstock, L., Macdonald, C., Wayland, R., Dimmick, F. and Fishman, J.: Improving national air quality forecasts with satellite aerosol observations, B. Am. Meteorol. Soc., 86, 1249–1261, 2005.

Borge, R., Lumbreras, J., Vardoulakis, S., Kassomenos, P., Rodr ǵuez, E.: Analysis of long-range transport influences on urban PM_{10} using two-stage atmospheric trajectory clusters, Atmos. Environ., 41, 4434-4450, 2007.

Chen, Z. H., Cheng, S. Y., Li, J. B., Guo, X. R., Wang, W. H., Chen, D. S.: Relationship between atmospheric pollution processes and synoptic pressure patterns

in northern China, Atmos. Environ., 42, 6078-6087, 2008a.

Chen, X. L., Fan, S. J., Li J. N., Liu, J., Wang, A. Y., Fong, S. K.: The typical weather characteristics of air pollution in Hong Kong area, J. Trop. Meteor., 24, 195-199, 2008b. (in Chinese)

Chen, Y., Zhao, C., Zhang, Q., Deng, Z., and Huang, M.: Aircraft study of Mountain Chimney Effect of Beijing, China, J. Geophys. Res., 114, D08306, doi:10.1029/2008JD010610, 2009.

Chen, S. Y., Huang, J. P., Fu, Q., Ge, J. M., Su, J.: Effects of aerosols on autumn precipitation over mid-eastern China, J. Trop. Meteor., 27, 339-347, 2012. (in Chinese)

Chen, B., Stein, A. F., Maldonado, P. G., Sanchez de la Campa, A. M., Gonzalez-Castanedo, Y., Castell, N., de la Rosa, J. D.: Size distribution and concentrations of heavy metals in atmospheric aerosols originating from industrial emissions as predicted by the HYSPLIT model, Atmos. Environ., 71, 234-244, 2013.

Chen, S., Zhao, C., Qian, Y., Leung, L. R., Huang, J., Huang, Z., Bi, J., Zhang, W. , Shi, J., Yang, L., Li, D., Li, J.: Regional modeling of dust mass balance and radiative forcing over East Asia using WRF-Chem, Aeolian Res., 15, 15–30, 2014.

Cheng, S. Y., Chen, D. S., Li, J. B., Wang, H. Y., Guo, X. R.: The assessment of emission-source contributions to air quality by using a coupled MM5-ARPS-CMAQ modeling system: a case study in the Beijing metropolitan region, China. Environ. Modell. Softw., 22, 1601-1616, 2007.

Chu, D. A., Kaufman, Y. J., Ichoku, C., Remer, L. A., Tanr ́e, D., and Holben, B. N.:

Validation of MODIS aerosol optical depth retrieval over land, Geophys. Res. Lett., 29, 8007, doi:10.1029/2001GL013 205, 2002.

Csavina, J., Field, J., Félix, O., Corral-Avitia, A. Y., Eduardo Sáez, A., Betterton, E. A.: Effect of wind speed and relative humidity on atmospheric dust concentrations in semi-arid climates, Sci. Total Environ, 487, 82-90, 2014.

Demuzere, M., Trigo, R. M., Vila-Guerau de Arellano, J., and van Lipzig, N. P. M.: The impact of weather and atmospheric circulation on O_3 and PM_{10} levels at a rural mid-latitude site, Atmos. Chem. Phys., 9, 2695-2714, doi:10.5194/acp-9-2695-2009, 2009.

Ding, A. J., Wang, T., Zhao, M., Wang, T., Li, Z.: Simulation of sea-land breezes and a discussion of their implications on the transport of air pollution during a multi-day ozone episode in the Pearl River Delta of China, Atmos. Environ., 38: 6737-6750, 2004.

Ding, A. J., Wang, T., Thouret, V., Cammas, J.-P., and Nédélec, P.: Tropospheric ozone climatology over Beijing: analysis of aircraft data from the MOZAIC program, Atmos. Chem. Phys., 8, 1-13, doi:10.5194/acp-8-1-2008, 2008.

Ding, A. J., Wang, T., Xue, L. K., Gao, J., Stohl, A., Lei, H. C., Jin, D. Z., Ren, Y., Wang, Z. F., Wei, X. L., Qi, Y. B., Liu, J., and Zhang, X. Q.: Transport of north China midlatitude cyclones: Case study of aircraft measurements in summer 2007, J. Geophys. Res., 114, D08304, doi:10.1029/2008JD011023, 2009.

Donaldson, K., Stone, V., Seaton, A., MacNee, W.: Ambient particle inhalation and the cardiovascular system: Potential mechanisms, Environ. Health. Persp., 109,

523-527, 2001.

Draxler, R. R., Hess, G. D.: Description of the HYSPLIT_4 modeling system, NOAA Technical Memorandum ERL ARL-224, 1997.

Flocas, H., Kelessis, A., Helmis, C., Petrakakis, M., Zoumakis, M., Pappas, K.: Synoptic and local scale atmospheric circulation associated with air pollution episodes in an urban Mediterranean area, Theor. Appl. Climatol., 95, 265-277, 2009.

Guo, J. P., Zhang, X. Y., Wu, Y. R., Zhaxi, Y. Z., Che, H. Z., La, B., Wang, W. and Li, X.W.: Spatio-temporal Variation Trends of Satellite-based Aerosol Optical Depth in China during 1980-2008, Atmos. Environ., 45, 6802–6811, 2011.

Guo, Y. F., Li, D. Y., Zhou, B., Xia, J., Wu, Y., Hu, Y. H.: Study on haze characteristics in Wuxi and its impact factors, Meteor. Mon., 39, 1314-1324, 2013. (in Chinese)

He, Q. S., Li, C. C., Geng, F. H., Lei, Y., Li, Y. H.: Study on long-term aerosol distribution over the land of east China using MODIS data, Aerosol Air Qual. Res., 12, 304-319, 2012.

Janssen, N. A., Hoek G., Simic-Lawson. M., Fischer, P., van Bree, L., ten Brink, H., Keuken, M., Atkinson, R. W., Anderson, H. R., Brunekreef, B. and Cassee, F. R.: Black carbon as an additional indicator of the adverse health effects of airborne particles compared with PM_{10} and $PM_{2.5}$, Environ. Health. Persp., 119, 1691–1699, 2011.

Kan, H., Chen, B.: Particulate air pollution in urban areas of Shanghai, China: health-based economic assessment, Sci. Total Environ., 322, 71–79, 2004.

Kassomenos, P. A., Sindosi, O. A., Lolis, C. J.andChaloulakou, A.: On the relation between seasonal synoptic circulation types and spatial air quality characteristics in Athens, Greece, J. Air. Waste. Manage., 53, 309–324, 2003.

Kaufman, Y. J., Tanre, D. and Boucher O.: A satellite view of aerosols in the climate system, Nature, 419, 215–223, 2002.

Kim, S. W., Yoon, S. C., Kim, J. Y. and Kim, S. Y.: Seasonal and monthly variations of columnar aerosol optical properties over East Asia determined from multi-year MODIS, LIDAR, and AERONET sun/sky radiometer measurements, Atmos. Environ., 41, 1634–1651, 2007.

Koren, I., Altaratz, O., Remer, L. A., Feingold, G., Martins, J. V., Heiblum, R. H.: Aerosol-induced intensification of rain from the tropics to the mid-latitudes, Nat. Geosci., 5(2): 118-122, doi: 10.1038/NGEO1364, 2012.

Li, Z. Q., Niu, F., Fan, J. W., Liu, Y. G., Rosenfeld, D., Ding, Y. N.: Long-term impacts of aerosols on the vertical development of clouds and precipitation, Nat. Geosci., 4(12): 888-894, doi: 10.1038/NGEO1313, 2011.

Lin, J., Nielsen, C. P., Zhao, Y., Lei, Y. Liu, Y. and Mcelroy, M. B.: Recent changes in particulate air pollution over China observed from space and the ground: effectiveness of emission control, Environ. Sci. and Technol., 44, 7771–7776, 2010.

Liu, Y. K., Liu, J. F., Tao, S.: Interannual variability of summertime aerosol optical depth over East Asia during 2000–2011: a potential influence from El Niño Southern Oscillation, Environ. Res. Lett., 8, 044034 , 2013.

Luo, Y. X., Zheng, X. B., Zhao, T. L., Chen, J.: A climatology of aerosol optical depth

over China from recent 10 years of MODIS remote sensing data, Int. J. Climatol., 34, 863-870, 2014.

Rosenfeld, D., Cattani, E., Melani, S., Levizzani, V.: Considerations on Daylight Operation of 1.6-VERSUS 3.7-μm Channel on NOAA and Metop Satellites, Bull. Amer. Meteor. Soc., 85(6): 873-881, 2004.

Rosenfeld, D., Dai, J., Yu, X., Yao, Z. Y., Xu, X. H., Yang, X., Du, C. L.: Inverse relations between amounts of air pollution and orographic precipitation, Science, 315(5817), 1396-1398,2007

Russo, A., Trigo, R. M., Martins, H., Mendes, M. T.: NO2, PM10 and O3 urban concentrations and its association with circulation weather types in Portugal, Atmos. Environ., 89, 768-785, 2014.

Saavedra, S., Rodr ǵuez, A., Taboada, J. J., Souto, J. A., Casares, J. J.: Synoptic patterns and air mass transport during ozone episodes in northwestern Iberia, Sci. Total Environ., 441, 97-110, 2012.

Shahgedanova, M., Burt, T. P., Davies, T. D.: Synoptic climatology of air pollution in Moscow, Theor. appl. climatol., 61, 85-102, 1998.

Tanner, P. A., Law, P. T.: Effects of synoptic weather systems upon the air quality in an Asian megacity, Water Air Soil Poll, 136, 105-124, 2002.

Twohy, C. H., Coakley, J. A. and Tahnk, W. R.: Effect of changes in relative humidity on aerosol scattering near clouds, J. Geophys. Res., 114, D05205, doi:10.1029/2008JD010991, 2009.

Twomey S.: The influence of pollution on the shortwave albedo of clouds, J. Atmos.

Sci., 34(7), 1149-1152,1977.

Wang, X. Q., Qi, Y. B., Wang, Z. F., Guo, H., Yu, T.: The influence of synoptic pattern on PM10 heavy air pollution in Beijing, Climatic Environ. Res., 12, 81-86, 2007. (in Chinese)

Wang, S. X., Zhang, C. Y,: Spatial and temporal distribution of air pollutant emissions from open burning of crop residues in China, Sciencepaper Online, 3, 329-333, 2008. (in Chinese)

Wang, J., Li, J. L., Zhang Y. H.: Weather situation classification and its feature in severe air pollution days in winter in Urumqi, J. Meteor. Environ., 29, 28-32, 2013. (in Chinese)

Wu, J., Guo, J., Zhao, D. M.: Characteristics of aerosol transport and distribution in East Asia, Atmos. Res., 132, 185-198, 2013.

Xin, J. Y., Zhang, Q., Wang, L. L., Gong, C. S., Wang, Y. S., Liu, Z. R. and Gao, W. K.: The empirical relationship between the PM 2.5 concentration and aerosol optical depth over the background of North China from 2009 to 2011, Atmos. Res., 138, 179-188, 2014.

Xu, W. Y., Zhao, C. S., Ran, L., Deng, Z. Z., Liu, P. F., Ma, N., Lin, W. L., Xu, X. B., Yan, P., He, X., Yu, J., Liang, W. D., and Chen, L. L.: Characteristics of pollutants and their correlation to meteorological conditions at a suburban site in the North China Plain, Atmos. Chem. Phys., 11, 4353-4369, doi:10.5194/acp-11-4353-2011, 2011.

Zhang, L., Liao, H., Li, J. P.: Impacts of Asian summer monsoon on seasonal and interannual variations of aerosols over eastern China, J. Geophys. Res., 115, D00K05,

doi:10.1029/2009JD012299, 2010.

Zhao, C., Wang, Y., Yang, Q., Fu, R., Cunnold, D., Choi, Y.: Impact of East Asian summer monsoon on the air quality over China: View from space, J. Geophys. Res., 115, D09301, doi:10.1029/2009JD012745, 2010.

Zhao, C., Liu, X., Leung, L. R.: Impact of the Desert dust on the summer monsoon system over Southwestern North America, Atmos. Chem. Phys., 12, 3717-3731, 2012.

Zhao, C., Leung, L. R., Easter, R., Hand, J., Avise, J.: Characterization of speciated aerosol direct radiative forcing over California, J. Geophys. Res., 118, 2372–2388, doi:10.1029/2012JD018364, 2013a.

Zhao, C., Liu, X., Qian, Y., Lin, G., McFarlane, S., Yoon, J., Wang, H., Hou, Z., Yang, B., Ma, P., Yan, H., Bao, J.: Sensitivity of Radiative Fluxes at Top of Atmosphere to Cloud-Microphysics and Aerosol Parameters in the Community Atmosphere Model (CAM5), Atmos. Chem. Phys., 13, 10969-10987, 2013b.

Zhao, C. S., Tie, X. X., Lin, Y. P.: A possible positive feedback of reduction of precipitation and increase in aerosols over eastern central China, Geophys. Res. Lett., 33, L11814, doi:10.1029/2006GL025959, 2006a.

Zhao, C. S., Tie, X. X., Brasseur, G., Noone, K. J., Nakajima, T., Zhang, Q., Zhang, R. Y., Huang, M. Y., Duan, Y., Li, G. L., and Ishizaka, Y.: Aircraft measurements of cloud droplet spectral dispersion and implications for indirect aerosol radiative forcing, Geophys. Res. Lett., 33, L16809, doi:10.1029/2006GL026653,2006b.

Ziomas, I., Melas, D., Zerefos, C., Bais, A., Paliatsos, A.: Forecasting peak pollutant levels from meteorological variables, Atmos. Environ., 29, 3703-3711, 1995.

Tables and captions

Table 1. Short description for the observed meteorological fields features for 18 pollution episodes (The rows in the table with same capital letters in the parentheses indicate those episodes are affected by the similar circulation patterns in all the three atmospheric levels.).

episodes	Year(Date)	Surface	850hPa	500hPa
1(A)	2002(01-04)	Before the passage of a cold front	strong cold wind blow to south	NW flow
2(B)	2002(08-16)	Uniform pressure field	the rear of anticyclone	W-NW flow
3(C)	2002(24-26)	Periphery of the high pressure system centered in the Mongolia	the foreside of anticyclone	NW flow (behind the trough)
4(C)	2004(07-13)	Periphery of the high pressure system centered in the Mongolia	the foreside of anticyclone	NW flow (behind the trough)
5(D)	2004(18-22)	Periphery of the high pressure system centered in the TP	anticyclonic circulation	W flow
6(F)	2004(27-29)	The rear of high pressure system	South wind	SW flow
7(D)	2005(16-18)	Periphery of the high pressure system centered in the TP	anticyclonic circulation	Shallow trough
8(E)	2005(23-26)	The rear of high pressure system	the rear of anticyclone	W-NW flow
9(B)	2006(04-15)	Uniform pressure field	the rear of anticyclone	W-NW flow
10(D)	2006(28-31)	Periphery of the high pressure system centered in the TP	the foreside of anticyclone	Shallow trough
11(B)	2007(16-25)	Uniform pressure field	anticyclonic circulation	W-NW flow
12(B)	2008(01-03)	Uniform pressure field	the rear of anticyclone	NW flow
13(E)	2008(13-17)	The rear of high pressure system	the rear of anticyclone	W-NW flow
14(C)	2009(02-06)	Periphery of the high pressure system centered in the Mongolia	the foreside of anticyclone	NW flow (behind the trough)
15(A)	2009(15-16)	Before the passage of a cold front	strong cold flow toward south	NW flow
16(D)	2009(21-25)	Periphery of the high pressure system centered in the TP	anticyclonic circulation	W flow
17(B)	2010(16-17)	Periphery of the high pressure system centered in the Mongolia	the rear of anticyclone	NW flow
18(C)	2010(28-31)	Periphery of the high pressure system centered in the Mongolia	the foreside of anticyclone	NW flow (behind the trough)

Table 2. As in Table 1, but for 10 pollution episodes.

episodes	Year(Date)	Surface	850hPa	500hPa
1(G)	2001(10-11)	Periphery of the high pressure system	anticyclonic circulation	NW flow (behind the trough)
2(H)	2001(29-30)	the rear of high pressure system	anticyclonic circulation	W flow
3(G)	2003(15-18)	Periphery of the high pressure system	the foreside of anticyclone, strong wind	NW flow
4(G)	2003(21-24)	Periphery of the high pressure system	the foreside of anticyclone, strong wind	NW flow
5(G)	2003(27-29)	Periphery of the high pressure system	the foreside of anticyclone, strong wind	NW flow
6(G)	2004(02-04)	Uniform pressure field	anticyclonic circulation	NW flow (behind the trough)
7(H)	2005(08-10)	the rear of high pressure system	anticyclonic circulation	W flow
8(I)	2008(23-26)	The passage of cold front	strong cold wind	NW flow
9(I)	2009(17-20)	The passage of cold front	strong cold wind	NW flow
10(G)	2010(03-04)	Periphery of the high pressure system	anticyclonic circulation, strong wind	NW flow (behind the trough)

Figures and captions

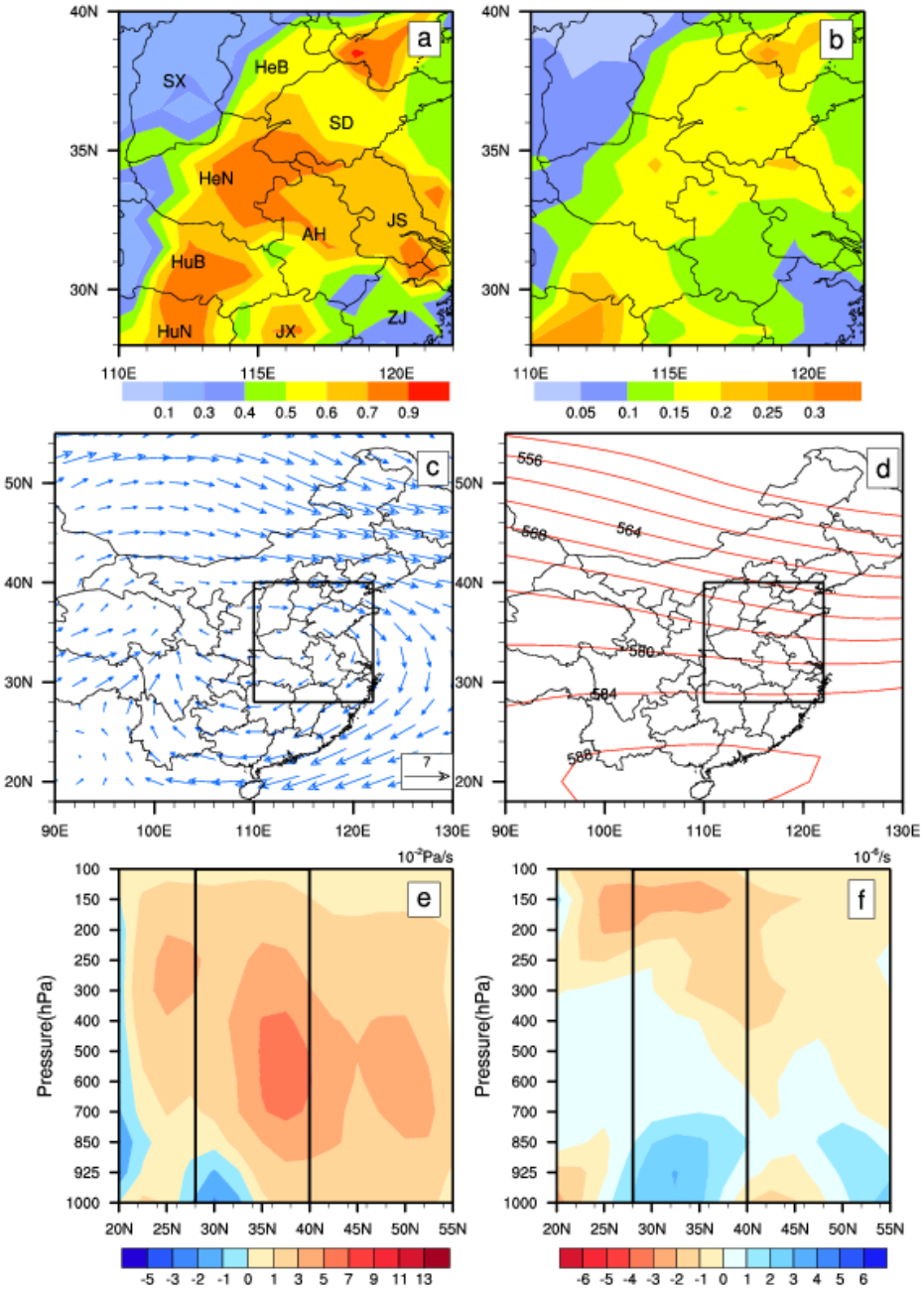

Fig.1. The mean distribution of (a) aerosol optical depth (AOD); (b) the standard deviation of AOD; (c)850hPa winds field; (d) 500hPa geopotential height field (e) height-latitude cross-sections of vertical velocity (10^{-2} Pa/s) and (f) divergence of winds (10^{-6}/s) averaged from longitude of 110°E-122°E in October for the period from 2001 to 2010.(Black letters on Fig.1.(a) indicate the different provinces. SX: Shanxi; SD: Shandong; HeB: Hebei; HeN: Henan; HuB: Hubei; HuN: Hunan; AH: Anhui; JX: Jiangxi; JS: Jiangsu; ZJ: Zhejiang.) Note: black rectangular region in (c) and (d) represents the East China (110°E-122°E, 28°N-40°N) and rectangular region in (e) and (f) represents the region 28°N-40°N.

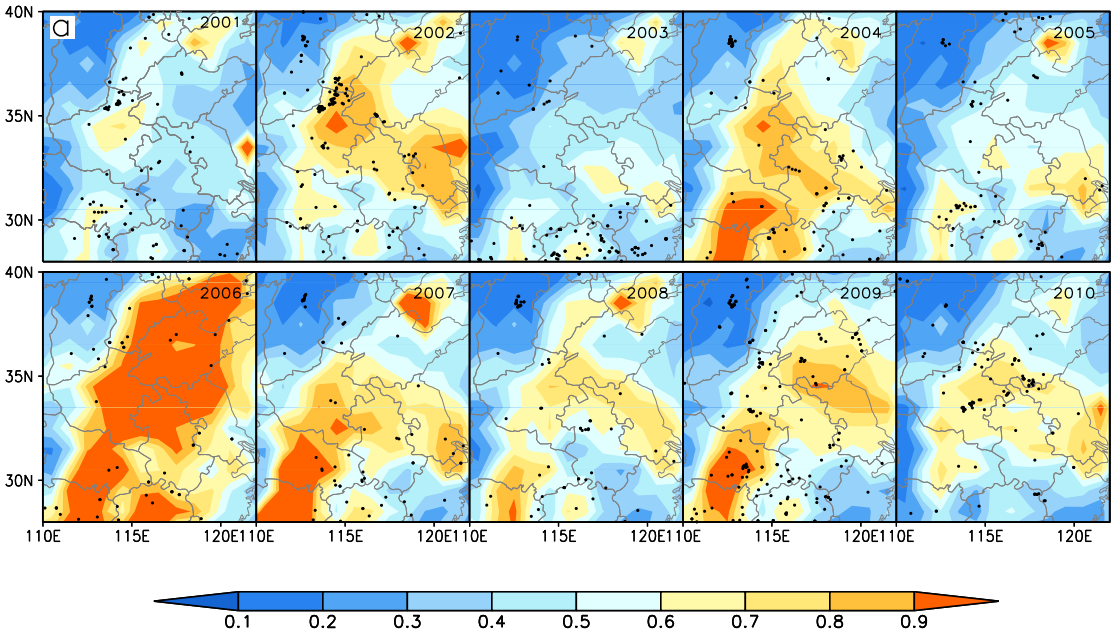

Fig. 2a. The distribution of AOD over East China in October for 2001-2010, the black dots are fire locations .

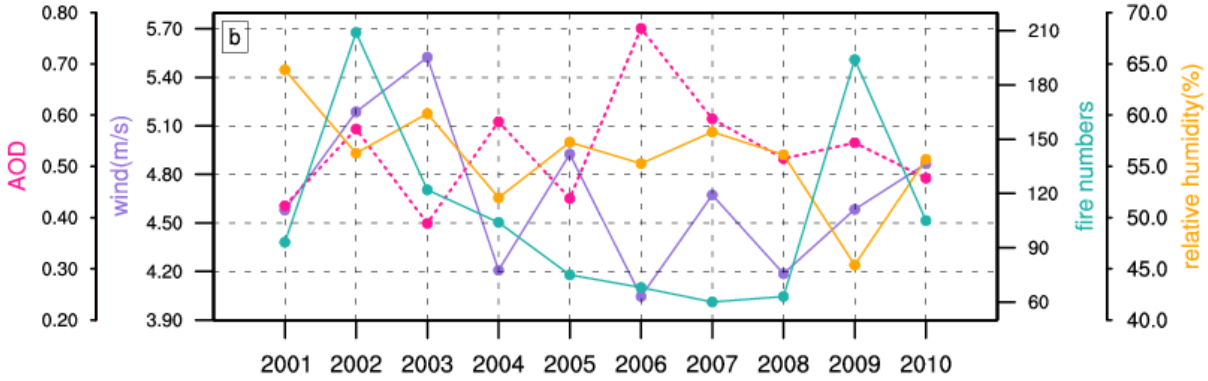

Fig.2b. Interannual variability of column AOD (peach); fire numbers (green); wind speed (purple) and relative humidity (orange) in the lower troposphere (1000hPa-850hPa), which are averaged over the region shown in 2a.

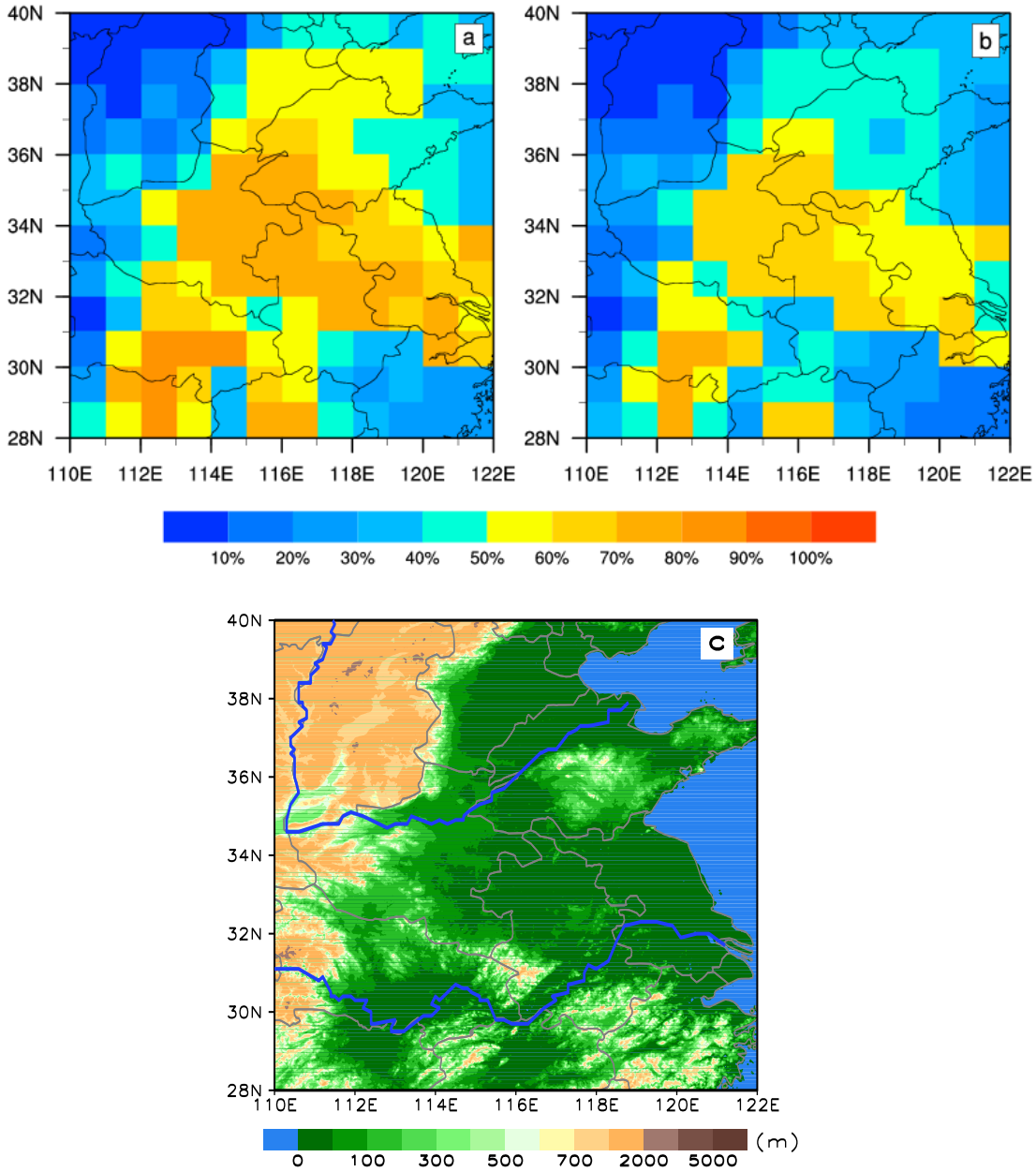

Fig.3. Frequency distribution of (a) AOD>0.5 and (b) AOD>0.6 in October calculated from 2001 to 2010, (c) the topography of East China.

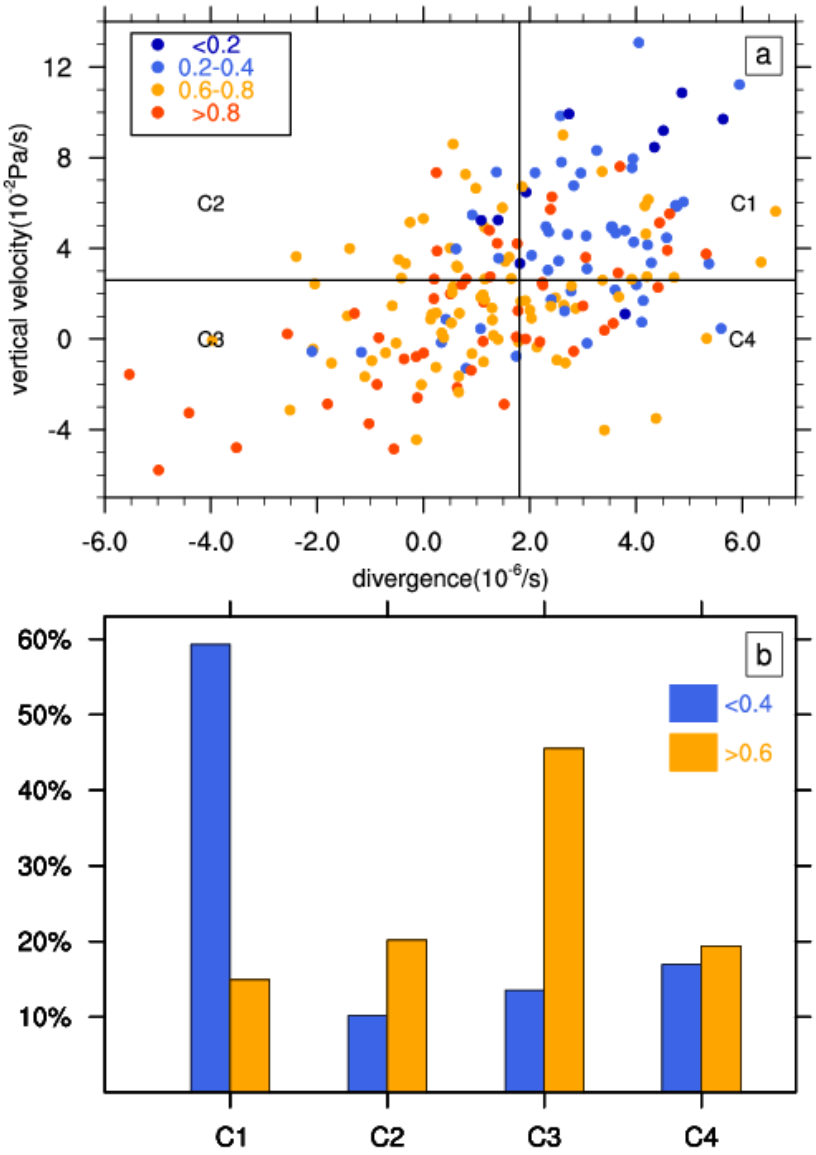

Fig. 4. (a) Dependence of AOD on vertical velocity (V:10^{-2}Pas^{-1}) averaged from 1000hPa to 100hPa and divergence of wind field (D: 10^{-6}s^{-1}) averaged from 1000hPa to 850hPa.The vertical black line stands for the climatological mean divergence (1.79×10^{-6}s^{-1}) and the horizontal line represents for that of vertical velocity (2.56×10^{-2} Pas^{-1}), the samples are divided into four categories according these two values.(C1 (D>1.79×10^{-6}; V>2.56×10^{-2}); C2(D<1.79×10^{-6};V>2.56×10^{-2});C3(D<1.79×10^{-6};V<2.56×10^{-2});C4(D>1.79×10^{-6};V<2.56×10^{-2}) .). (b): Frequency distribution of AOD>0.6 and AOD<0.4 for each category.

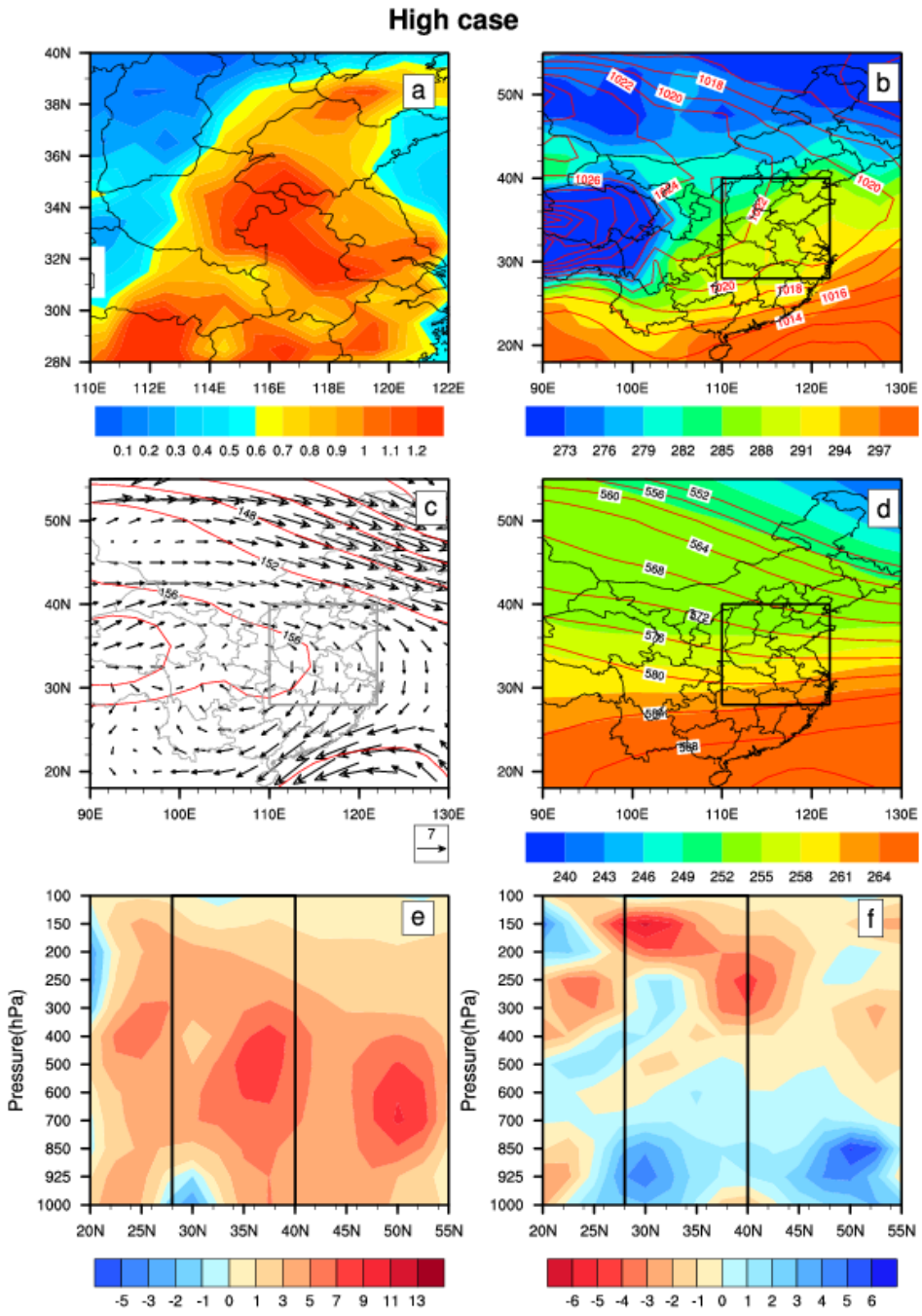

Fig. 5. One typical polluted episode (28th.Oct.2006 to 31st.Oct.2006). (a) the distribution of AOD over East China (b) sea level pressure (red line) and temperature (color shades) fields;; (c) 850hPa wind and geopotential height (red line) fields; (d) 500hPa temperature (color shades) and geopotential height (red line) fields; (e) height-latitude cross-sections of vertical velocity (10^{-2} Pa per second) and (f) divergence of winds (10^{-6} per second) averaged from longitude of 110°E-122°E. Note: black rectangular region represents the East China (110°E-122°E, 28°N-40°N).

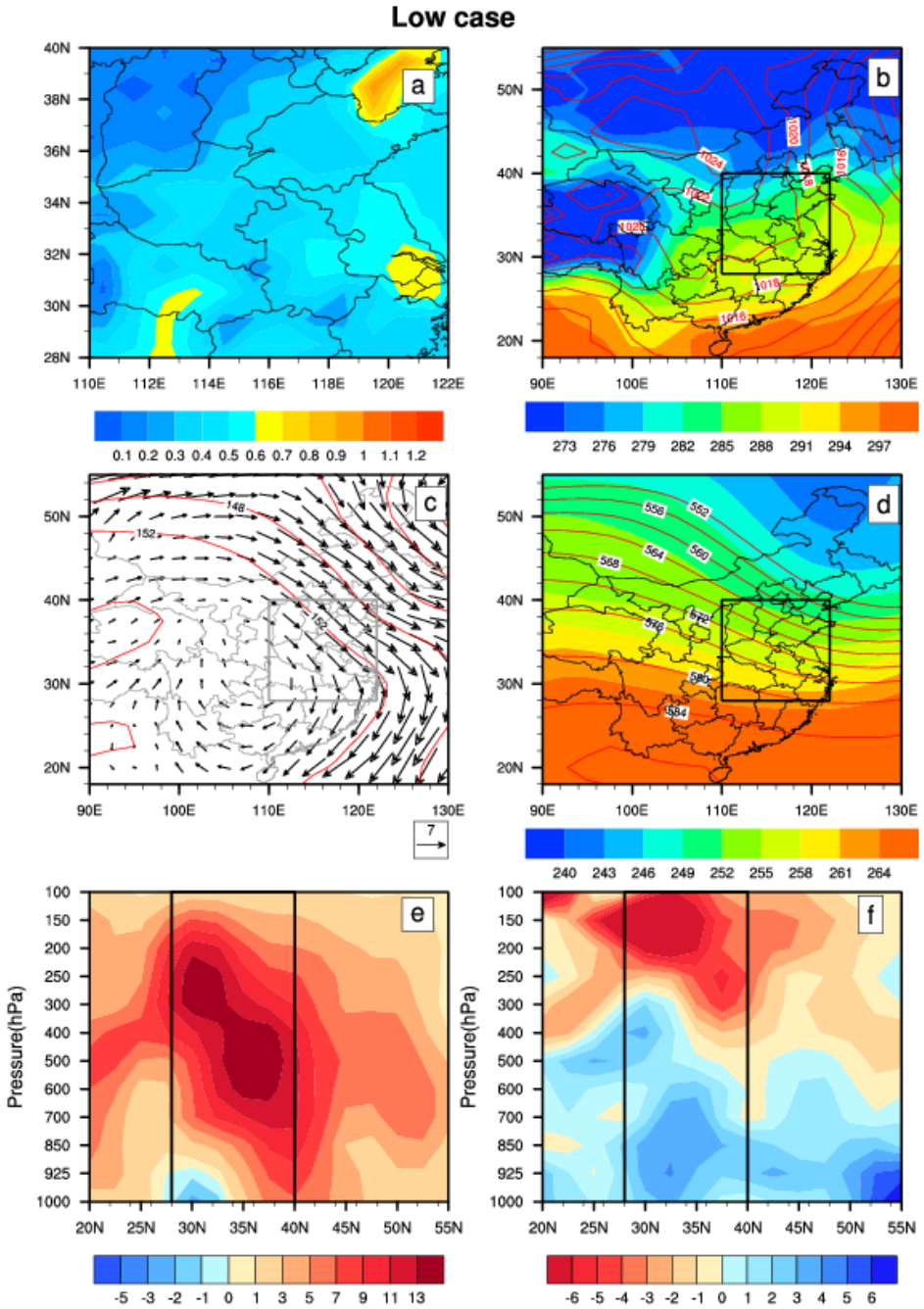

Fig. 6. As in Fig.5, but for the clean episode (21st.Oct.2003 to 24th.Oct.2003)

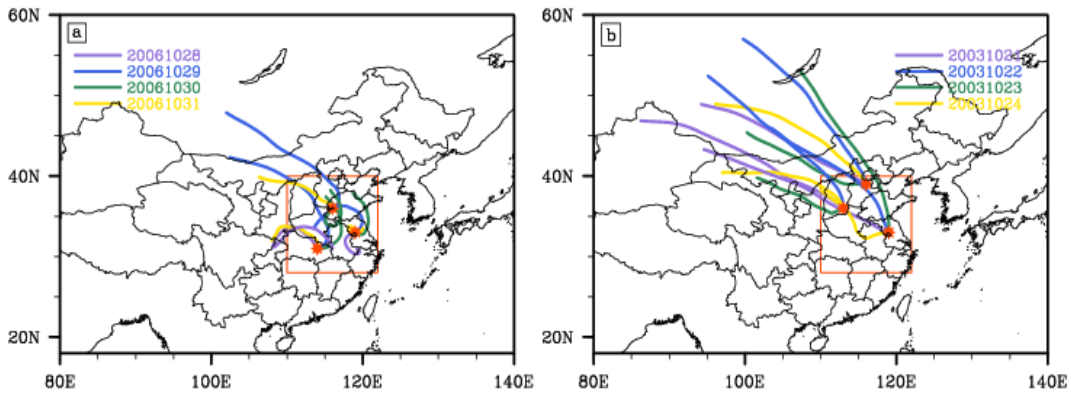

Fig. 7. The 48-hour backward trajectories for two episodes over East China (red box), three red star represent three ending points: (a) pollution episode, at 31 °N,114 °E; 33 °N,119 °E; 36 °N,116 °E. (b) clean episode, at 33 °N,119 °E; 36 °N,113 °E; 39 °N,116 °E.

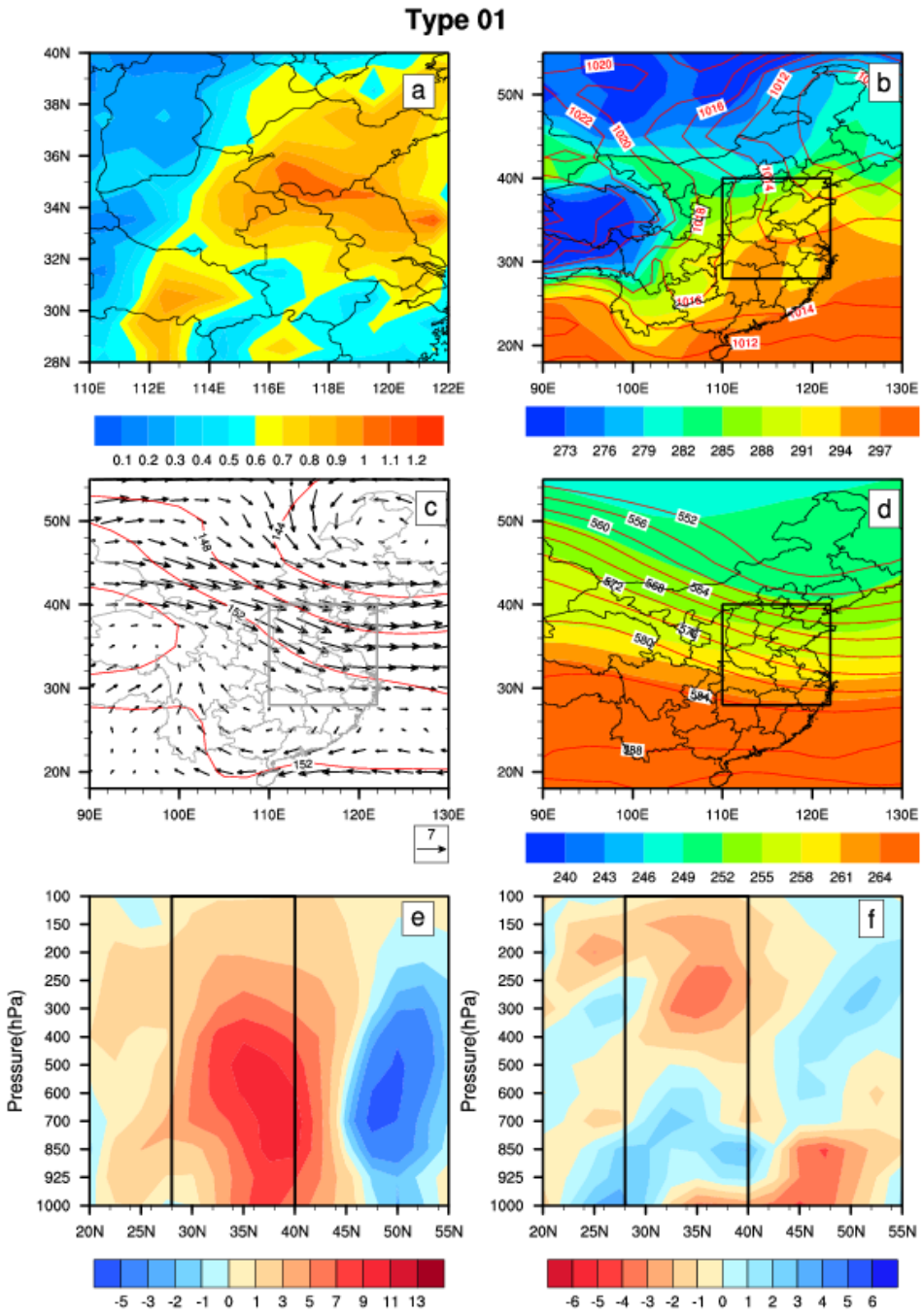

Fig. 8. Type 1 (polluted): (a) the distribution of AOD over East China (b) sea level pressure (red line) and temperature (color shades) fields; (c) 850hPa wind field and geopotential height (red line) fields; (d) 500hPa temperature (color shades) and geopotential height (red line) fields; (e) height-latitude cross-sections of vertical velocity (10^{-2} Pa per second) and (f) divergence of winds (10^{-6} per second) averaged from longitude of 110°E-122°E. Note: black rectangular region represents the East China (110°E-122°E, 28°N-40°N).

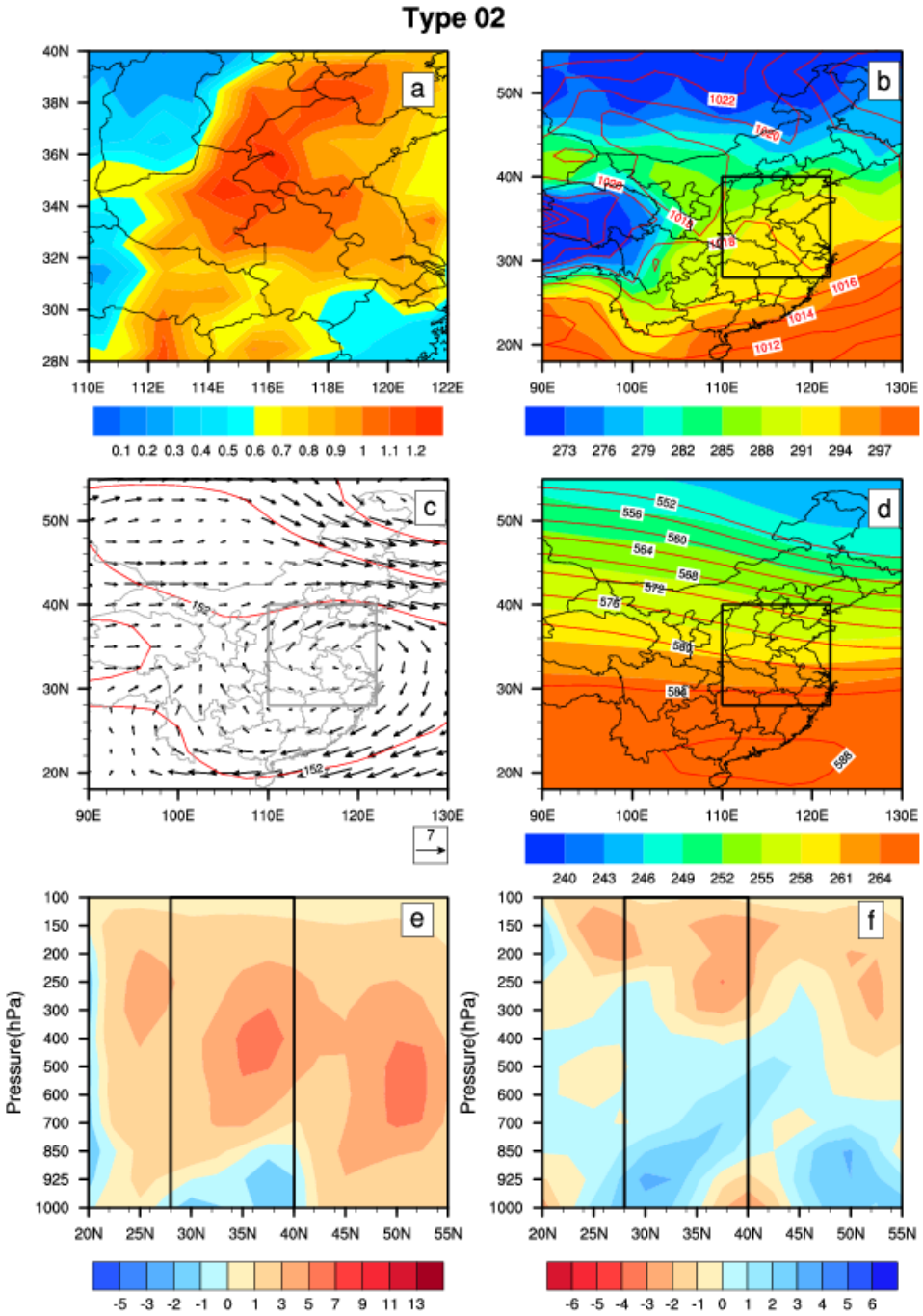

Fig. 9. As in Fig.8, but for the type 2 (polluted).

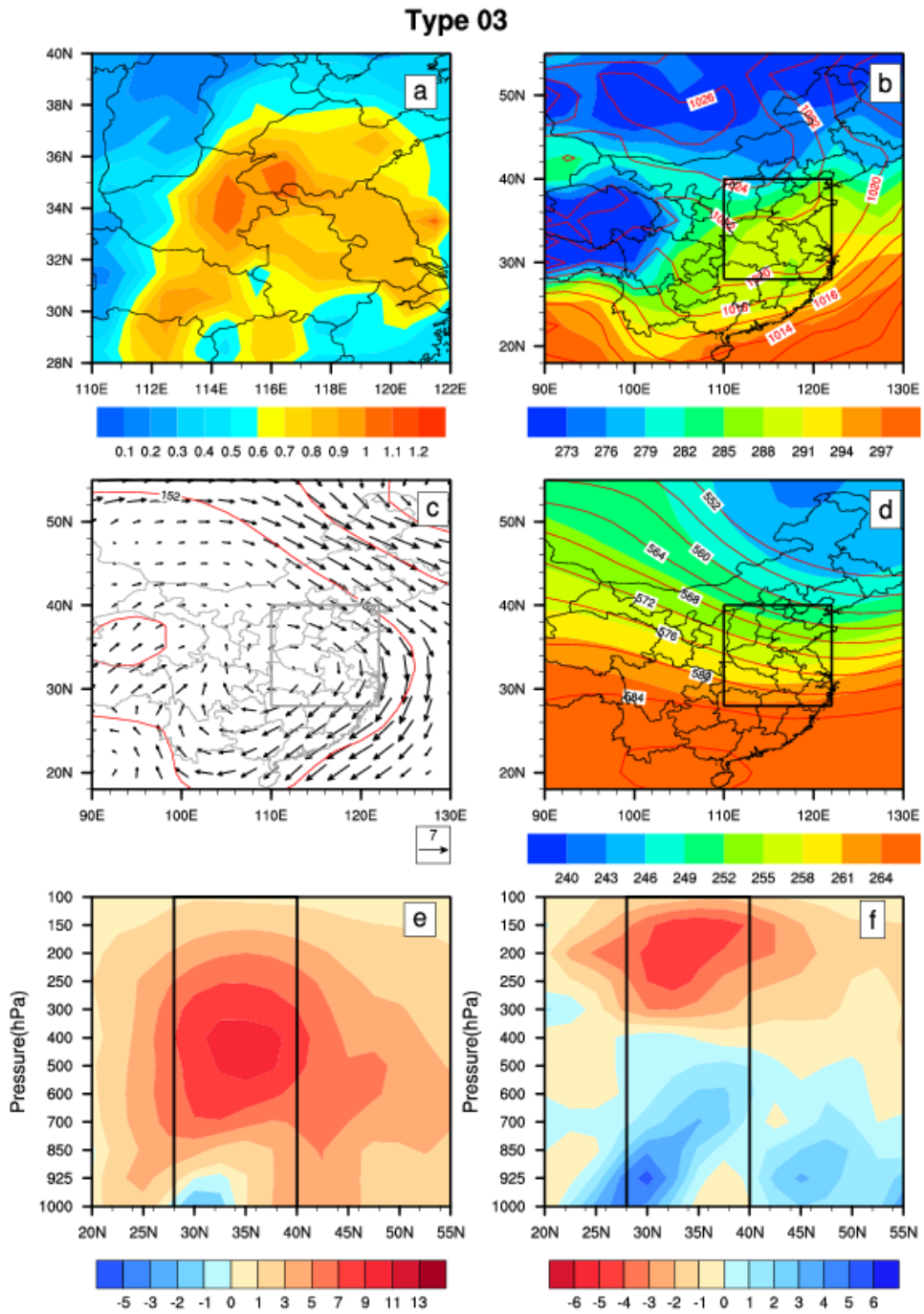

Fig. 10. As in Fig.8, but for the type 3 (polluted).

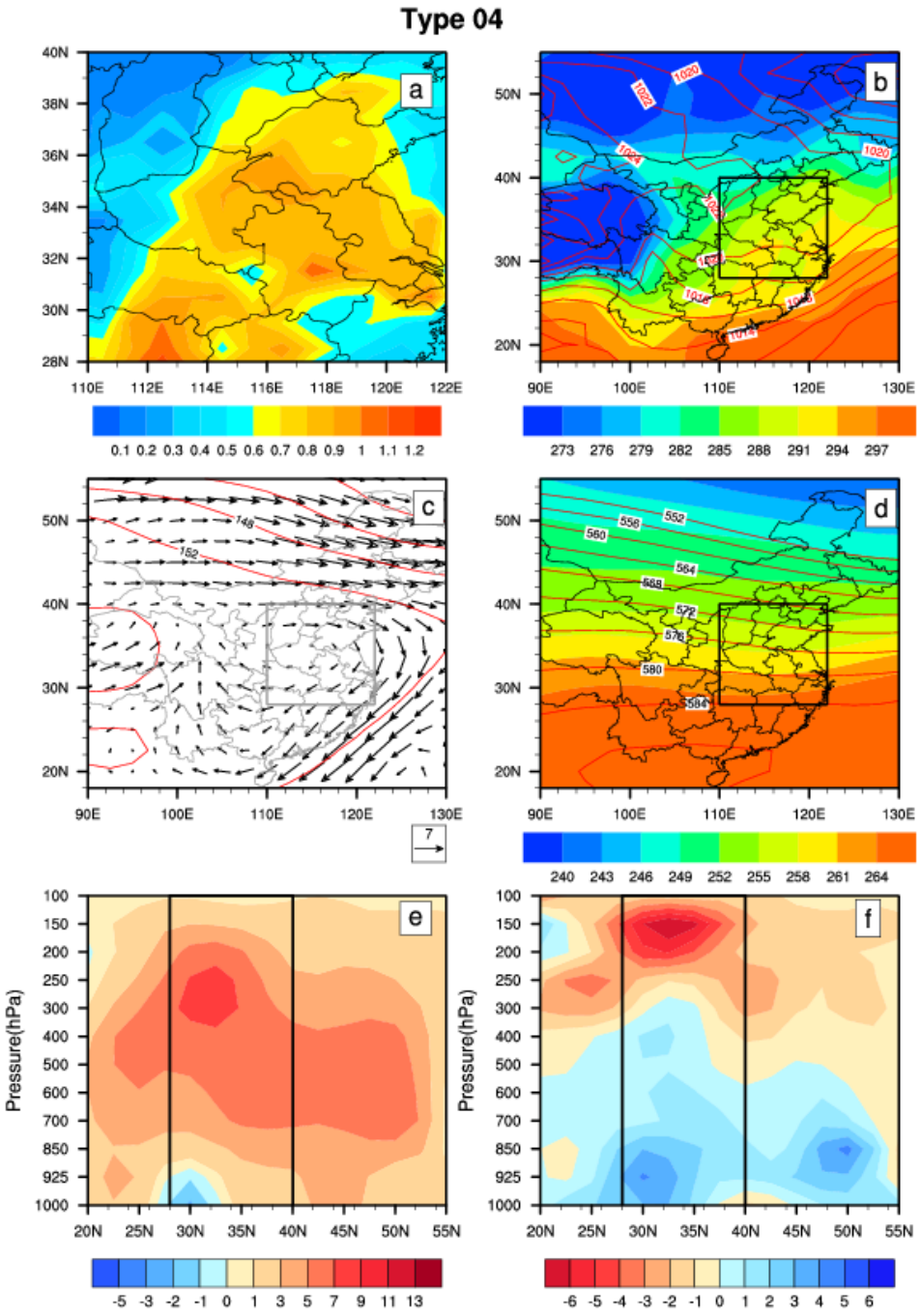

Fig.11. As in Fig.8, but for the type 4 (polluted).

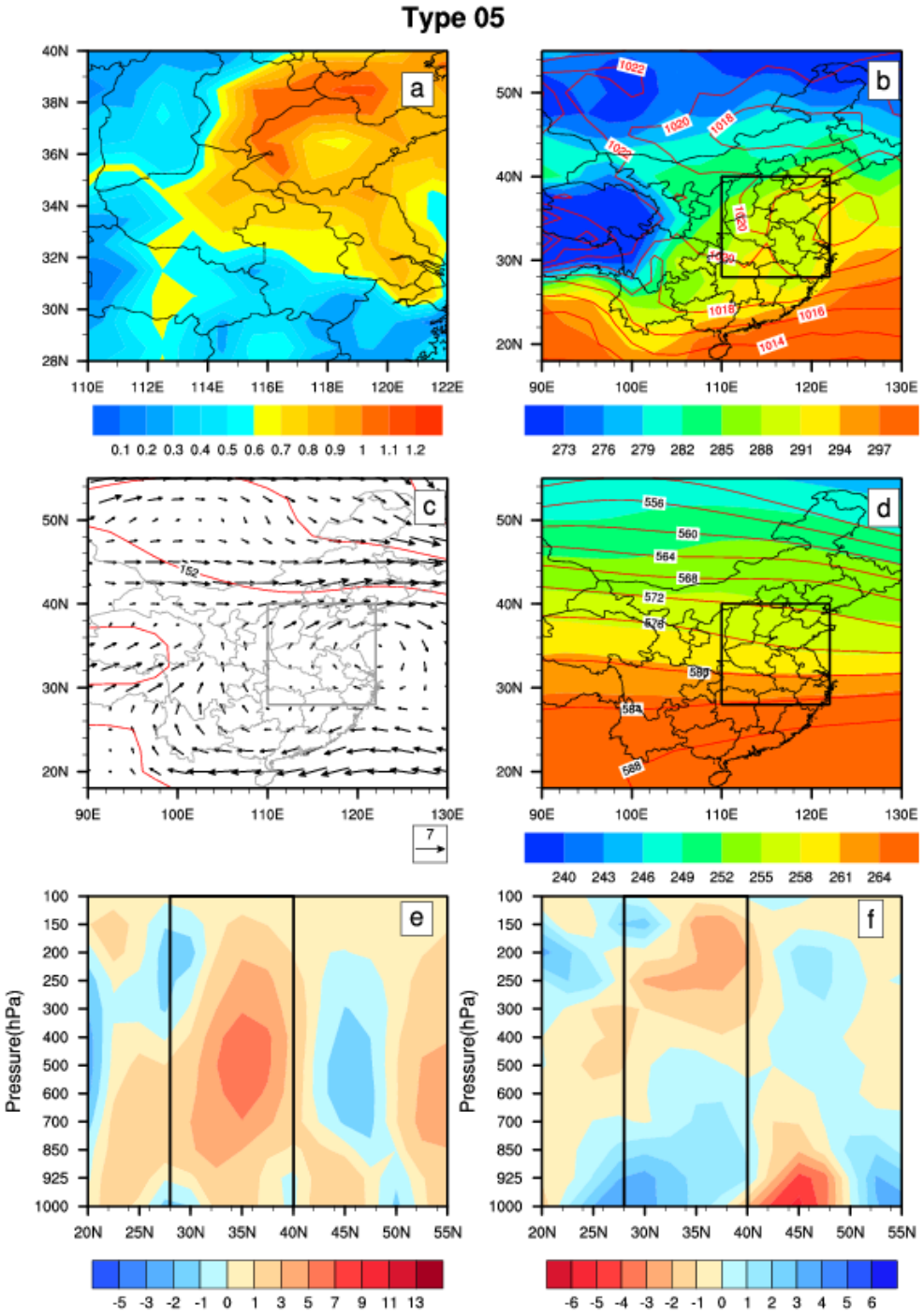

Fig.12. As in Fig.8, but for the type 5 (polluted).

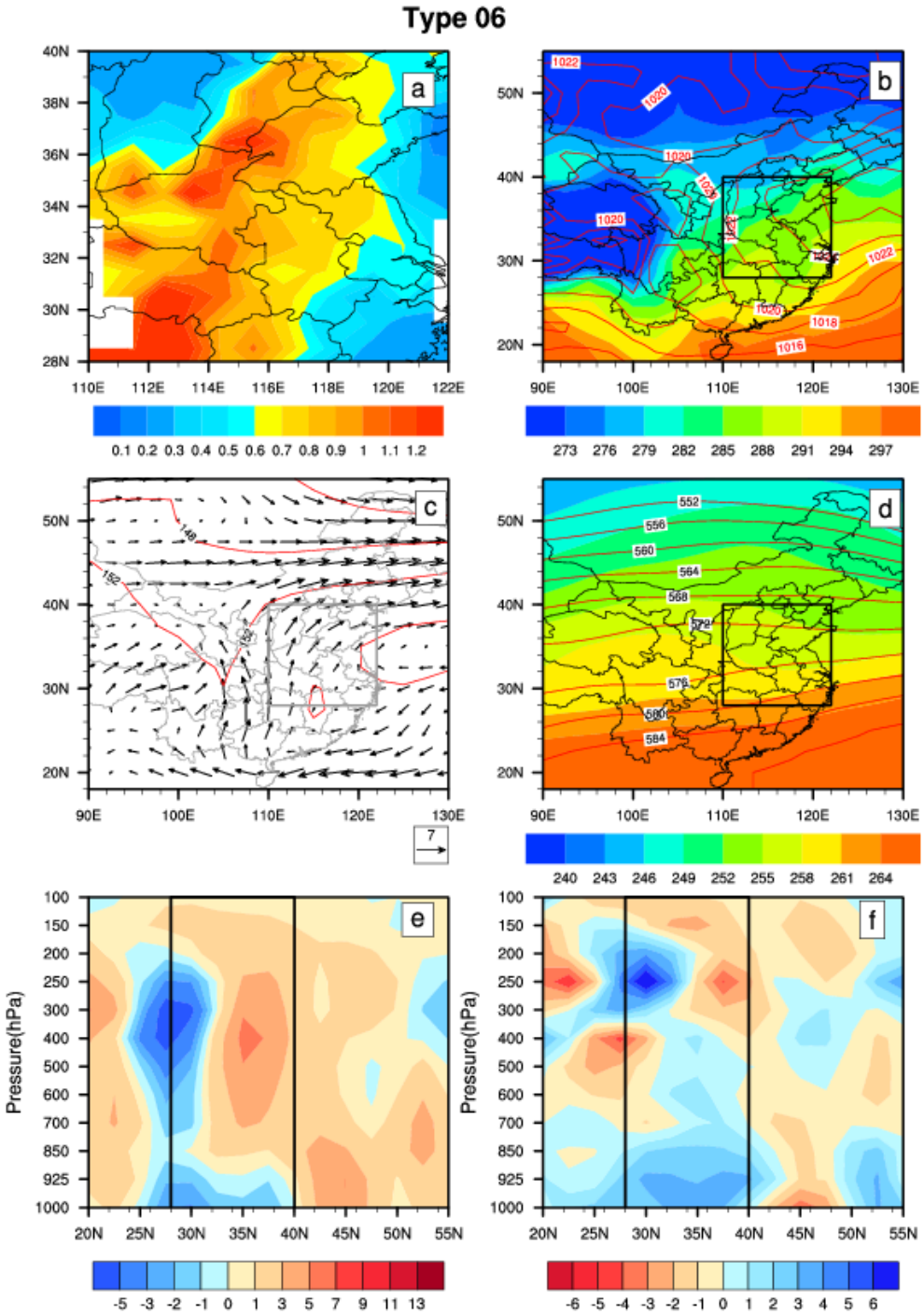

Fig.13. As in Fig.8, but for the type 6 (polluted).

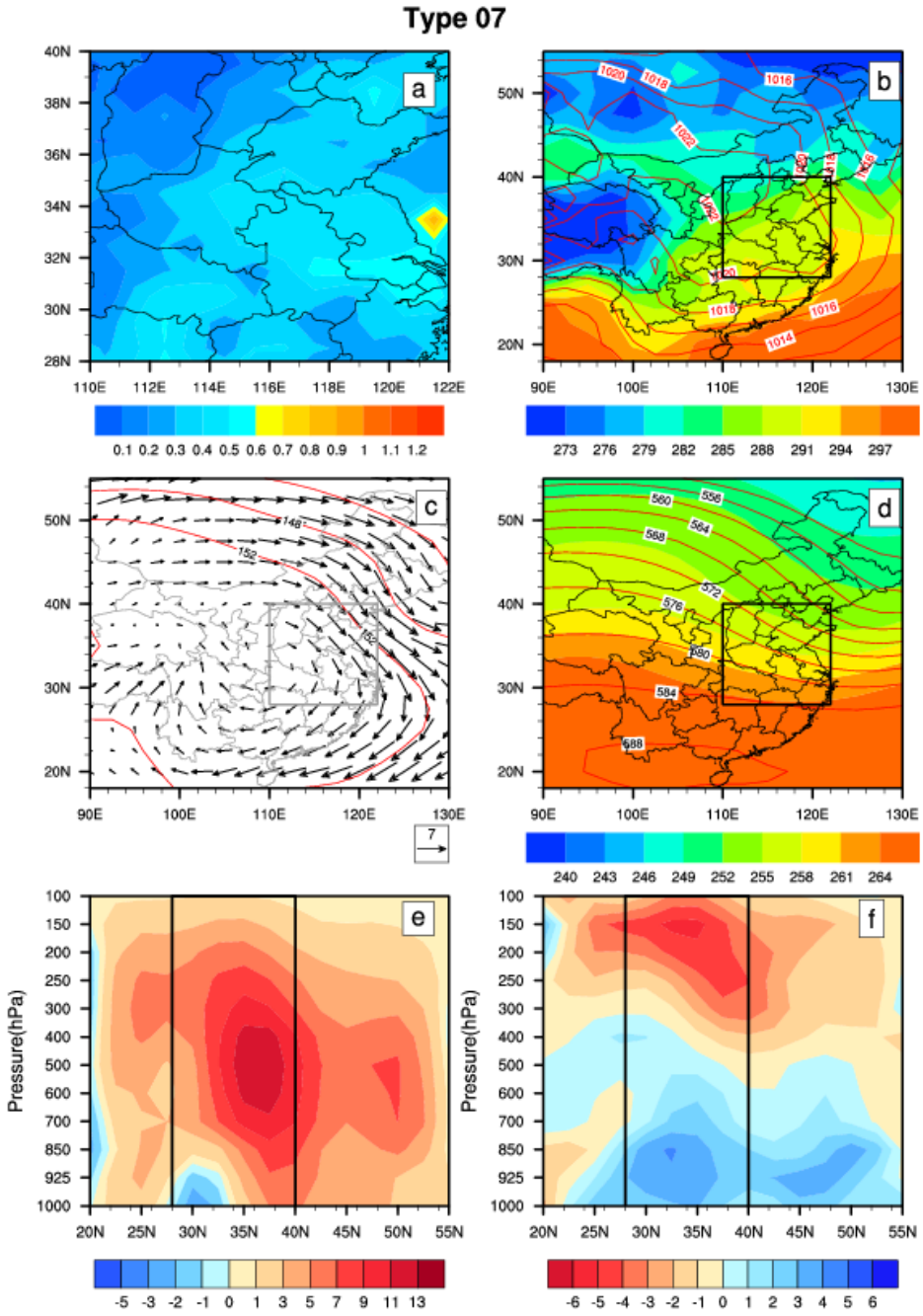

Fig.14. As in Fig.8, but for the type 7 (clean).

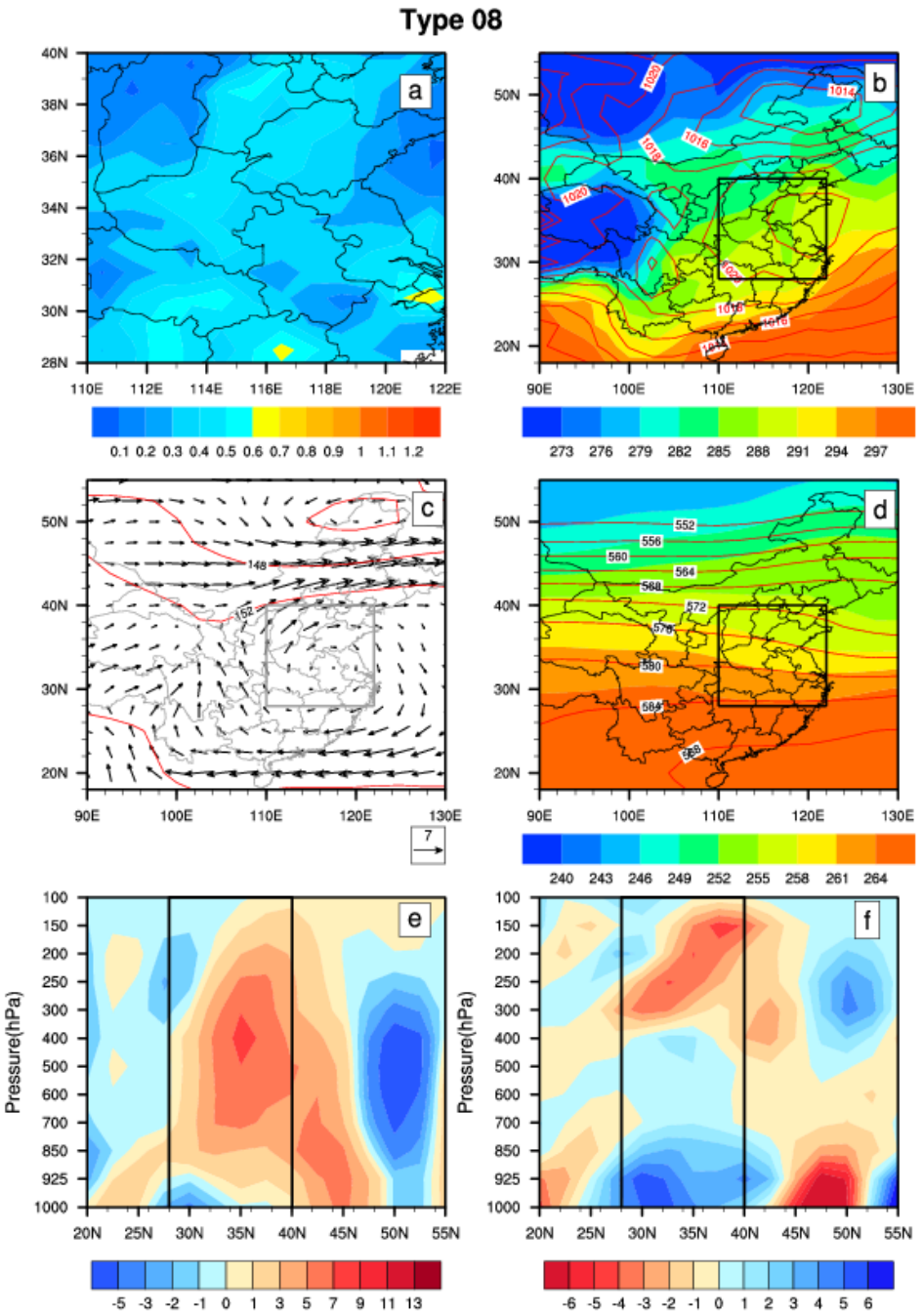

Fig.15. As in Fig.8, but for the type 8 (clean).

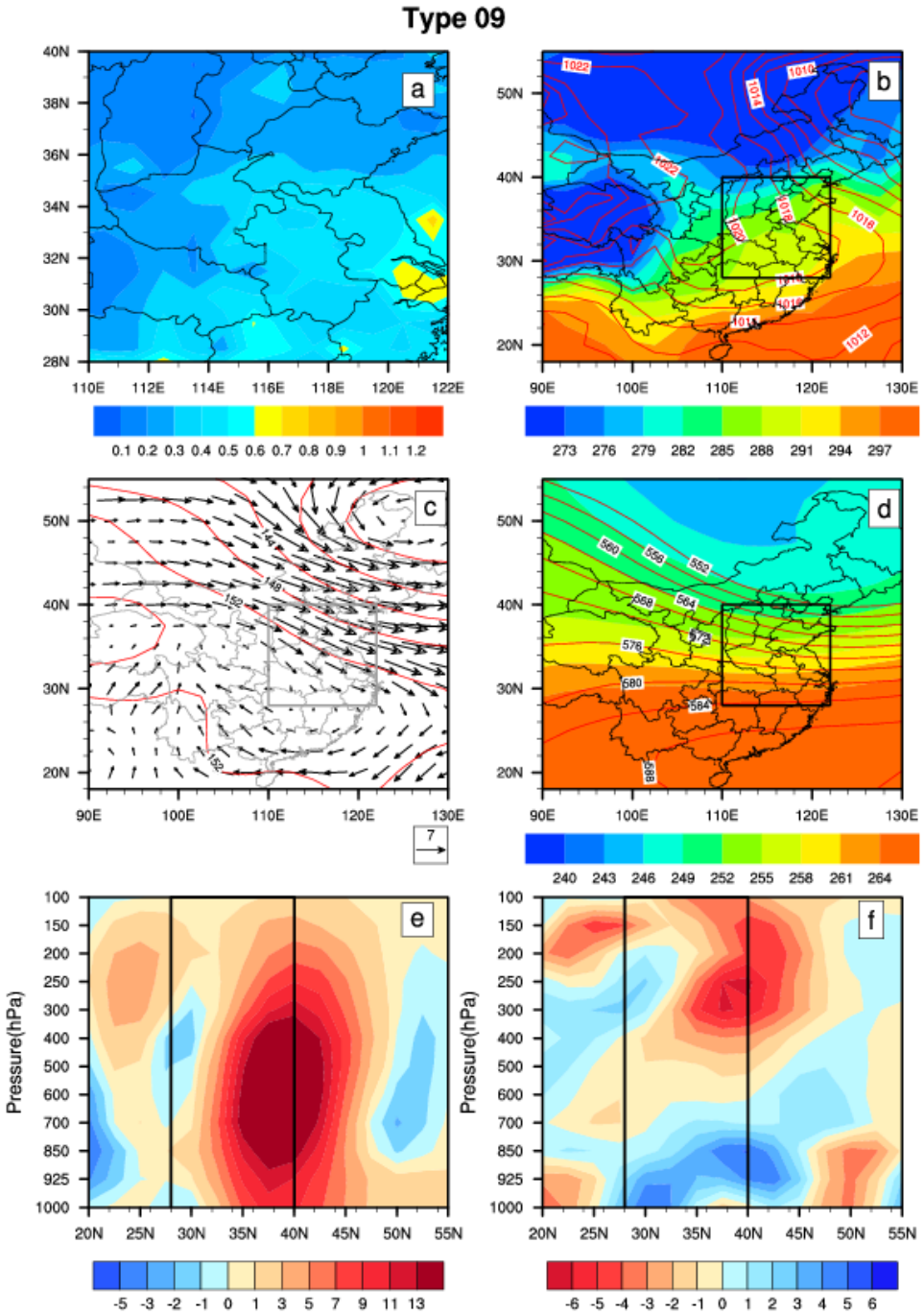

Fig.16. As in Fig. 8, but for the type 9 (clean).

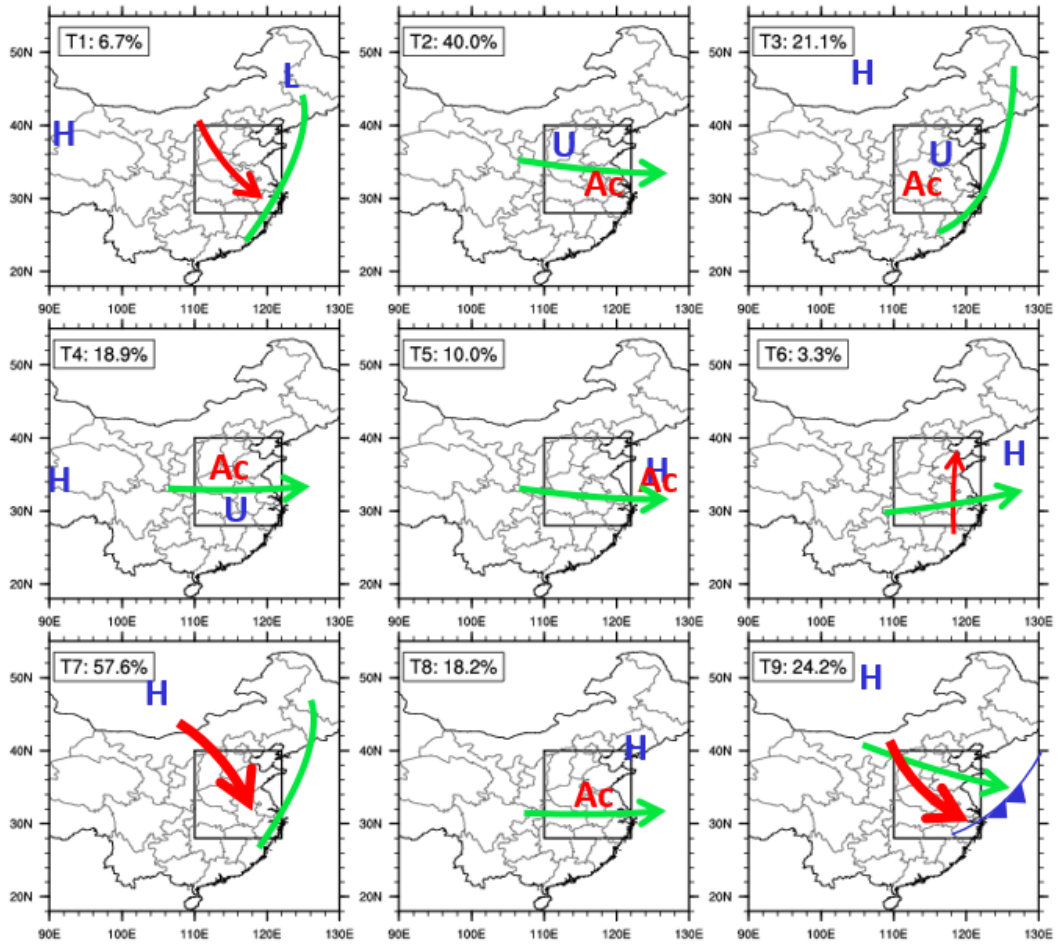

Fig.17. Schematic diagram of nine circulation types. The surface, 850hPa level and 500hPa level are shown by blue, red and green marks respectively. Note: At surface, “H/L” is the location of high/low pressure centre; “U” means a uniform pressure field in East China; At 850hPa, “Ac” represents for the existence of an anticyclone, or else the red arrow is used to indicate the wind direction and speed. At 500hPa, the green marks are used to indicate the direction of upper air flow or the location of trough line.

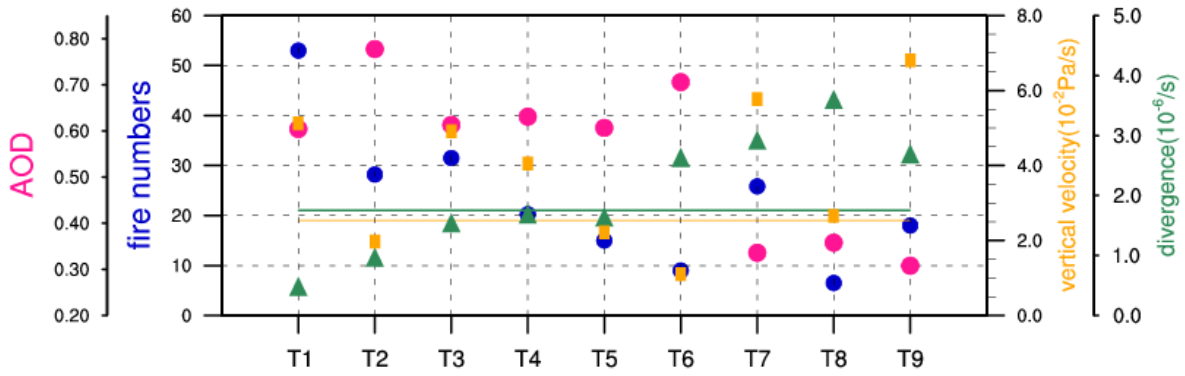

Fig.18. The value of AOD (peach); fire numbers (blue); vertical velocity (orange) and divergence of low level winds (green). The orange and green line represent for the climatological average of vertical velocity and divergence respectively.